Computer Modeling in Engineering & Sciences

Tech Science Press

https://doi.org/10.32604/cmes.2026.076683

ARTICLE

Quantum-Optimization-Based Clustering and Routing Protocols for Energy-Efficient, Scalable Wireless Sensor Networks

Amjad Rehman[1], **Tariq Mahmood**[1,2], **Faten S. Alamri**[3,*] **and Muhammad I. Khan**[1]

[1]Artificial Intelligence and Data Analytics (AIDA) Lab, CCIS, Prince Sultan University, Riyadh, Saudi Arabia
[2]School of System and Technology, Department of Artificial Intelligence, University of Management and Technology, Lahore, Pakistan
[3]Department of Mathematical Sciences, College of Science, Princess Nourah bint Abdulrahman University, Riyadh, Saudi Arabia

*Corresponding Author: Faten S. Alamri. Email: fsalamri@pnu.edu.sa

Received: 25 November 2025; Accepted: 31 March 2026; Published: 27 May 2026

ABSTRACT: The rapid deployment of Wireless Sensor Networks (WSNs) faces critical challenges due to sensor nodes' limited energy and communication capabilities, which restrict network lifetime and data transmission efficiency. Traditional clustering and routing protocols often lead to unbalanced energy consumption and uneven load distribution, whereas intelligent optimization approaches are hindered by high computational costs and slow convergence. This research formulates the clustering and routing problems in WSNs as an optimization challenge under resource and energy constraints, aiming to improve stability, energy efficiency, and throughput. This research proposed three quantum optimization-based solutions to address complex issues. First, a Quantum Genetic-Enhanced K-means (QGE-K) protocol addresses inaccurate cluster-head initialization by adaptively determining the optimal number of clusters and selecting energy-balanced cluster heads, thereby improving clustering accuracy and routing efficiency. Second, a Fuzzy-Enhanced Quantum Annealing Algorithm (FEQA) protocol integrates fuzzy inference with quantum tunneling dynamics to select cluster heads and compute the most energy-efficient routing paths, extending the network lifetime in large-scale deployments. Third, a Quantum-Enhanced Particle Swarm Clustering and Routing (QE-PSCR) protocol encodes clustering and routing into a single optimization particle, employing chaotic mapping and Lévy flight strategies to accelerate convergence and escape local optima, thereby reducing computation overhead. The simulation results demonstrate that all three protocols achieve significant improvements in energy consumption, load balance, throughput, and overall network lifetime. The proposed methods apply to domains such as environmental monitoring, the industrial Internet of Things, and military security, highlighting both theoretical contributions and practical value in advancing energy-efficient WSN design.

KEYWORDS: Wireless sensor networks; quantum genetic-enhanced K-means; quantum annealing algorithm; chaotic mapping; energy consumption; load balancing

1 Introduction

Wireless Sensor Networks (WSNs) have become a fundamental technology for real-time monitoring and data acquisition in diverse application domains, including environmental surveillance, healthcare systems, industrial Internet of Things (IoT), and military operations [1]. A typical WSN consists of a large number of low-power sensor nodes that collaboratively sense environmental data and transmit the collected information to a central base station (BS). However, these sensor nodes operate under strict constraints in terms of energy, computation, and communication resources, and they are often powered by non-replaceable

batteries [2]. Consequently, energy efficiency and network lifetime extension remain major design challenges in WSNs.

Clustering-based routing protocols are widely used to address these challenges by organizing nodes into clusters, where cluster heads (CHs) perform data aggregation and forward the collected information to the BS [3]. This hierarchical communication structure reduces redundant transmissions and improves network scalability. Nevertheless, traditional clustering protocols often suffer from uneven cluster-head distribution, unbalanced energy consumption, and premature node failures, which ultimately degrade network stability and efficiency [4].

To mitigate these limitations, various metaheuristic optimization algorithms, including Genetic Algorithms (GA), Ant Colony Optimization (ACO), and Firefly Algorithms, have been applied to cluster-head selection and routing optimization [5]. These methods improve energy balancing and clustering efficiency but often encounter issues such as slow convergence, high computational overhead, and susceptibility to local optima. Recently, with advances in artificial intelligence and quantum-inspired computing, researchers have explored quantum-inspired optimization techniques to overcome these limitations [6]. Quantum-inspired algorithms exploit concepts such as superposition, probabilistic state representation, and tunneling-like search mechanisms, enabling more efficient exploration of complex solution spaces. Methods such as Quantum Genetic Algorithms, Quantum Annealing, and Quantum-Behaved Particle Swarm Optimization (QPSO) have demonstrated promising performance in solving large-scale optimization problems and avoiding premature convergence [7].

In practical WSN deployments, energy imbalance caused by uneven cluster-head distribution remains a major problem. Random node placement often leads to some CHs handling excessive communication loads, resulting in early energy depletion and reduced network lifetime [8]. Additionally, flat routing approaches struggle to scale effectively as network size increases, causing higher communication overhead and reduced throughput [9]. Therefore, the clustering and routing problem in WSNs can be formulated as a multi-objective optimization task, where the goal is to minimize energy consumption while balancing node workloads and maximizing network lifetime and data throughput [10].

To address these challenges, this study adopts a comprehensive modeling framework consisting of three supporting components: a system model, an energy consumption model, and a network performance model. The system model assumes a homogeneous WSN where static sensor nodes are randomly deployed within a monitoring area, each having identical initial energy and communication capability. The base station is assumed to possess sufficient computational resources and unlimited energy. Data communication occurs through cluster-based routing, where nodes send sensed data to their respective CHs, and CHs forward aggregated data to the BS using either single-hop or multi-hop transmission [11]. The energy consumption model follows the widely used first-order radio model, which accounts for the energy required for transmission, reception, and data aggregation based on communication distance. Network performance is evaluated using metrics such as network lifetime, energy consumption, throughput, and load balance, which are commonly used to assess routing efficiency in WSNs [12].

Motivated by the limitations of existing clustering and routing methods, this work introduces quantum-inspired optimization techniques to improve energy efficiency and network lifetime in WSNs. Traditional protocols such as LEACH and HEED, as well as classical optimization approaches including GA and Particle Swarm Optimization (PSO), often struggle with local optima and uneven energy distribution in large-scale networks [13]. To overcome these issues, this paper proposes three quantum-inspired protocols: QGE-K, FEQA, and QE-PSCR, each designed to enhance different aspects of the WSN clustering and routing process.

The QGE-K protocol integrates K-means clustering with a Quantum Genetic Algorithm to improve cluster initialization and cluster-head selection, resulting in better clustering accuracy and balanced energy distribution. The FEQA protocol combines fuzzy inference for candidate CH selection with quantum annealing for routing optimization, enabling energy-efficient path selection and improved global routing performance. Finally, the QE-PSCR protocol employs quantum-behaved particle swarm optimization enhanced with chaotic initialization and Lévy flight strategies to jointly optimize clustering and routing decisions, enabling faster convergence and improved global search capability.

Although all three protocols are based on quantum-inspired optimization, they address different components of the WSN optimization problem. QGE-K primarily improves cluster formation, FEQA focuses on energy-efficient routing, and QE-PSCR performs integrated clustering–routing optimization. Consequently, the three approaches complement each other by targeting clustering enhancement, routing efficiency, and unified optimization, respectively. The proposed framework demonstrates the potential of quantum-inspired optimization techniques to improve energy utilization, balance network load, and extend network lifetime in WSNs. These contributions also highlight new opportunities for applying advanced optimization methods in IoT systems and large-scale real-time monitoring applications.

1.1 Key Research Challenges in Wireless Sensor Networks

This research addresses key limitations in WSNs by exploring quantum-inspired optimization techniques for clustering and routing. Traditional approaches often struggle with energy efficiency, computational complexity, and network performance.

- A major challenge in WSNs is the limited energy of sensor nodes, which are typically powered by non-replaceable batteries. Extending network lifetime is therefore a primary design objective [14]. Traditional clustering protocols often lead to unbalanced energy consumption, as cluster heads (CHs) handle additional communication and data aggregation tasks. Poor CH selection accelerates energy depletion and results in premature node failure and reduced network lifetime [15,16].
- Existing clustering and routing methods also face performance and scalability limitations. Many optimization-based approaches suffer from high computational complexity and slow convergence [17]. Classical techniques such as K-means are sensitive to random initialization, which can lead to inaccurate clustering. As network size increases, flat routing becomes inefficient, while hierarchical protocols may still struggle to maintain optimal performance in diverse deployment scenarios [18,19].
- Another limitation of existing optimization methods is their tendency to converge to local optima due to restricted search capability [20]. Additionally, WSNs operate in dynamic environments where node energy levels and network topology change over time. This requires adaptive clustering and routing strategies capable of maintaining energy balance and stable network performance [21].

1.2 Novel Contribution

The study presents novel solutions that leverage quantum optimization algorithms to address the key problems of unbalanced energy consumption, premature node failure, and scalability limitations in large-scale sensor networks. Our main contributions in this paper are:

- The proposed quantum-inspired algorithms provide scalable, energy-efficient alternatives for applications across general IoT and sensor environments, including environmental monitoring, industrial IoT systems, and defense communication networks.
- The hybrid clustering and routing framework (QGE-K) is based on a combination of the K-means algorithm and a QGA to identify the initial selection of cluster heads and the formation of clusters.

The proposed framework achieves better clustering accuracy than existing methods, reduces energy consumption, and improves routing stability for clustering protocols.

- The FEQA protocol is proposed to combine fuzzy inference abilities with a quantum annealer for energy-efficient routing paths. The overall energy consumption is significantly reduced through adaptive cluster-head selection and quantum-based routing path optimization, thereby improving network stability and prolonging operational lifetime in large-scale deployments.
- The proposed QE-PSCR protocol combines Quantum Particle Swarm Optimization (QPSO) with chaotic mapping and Lévy flight strategies to accelerate convergence and avoid local optima. The model jointly optimizes clustering and routing, achieving faster computation and reduced communication overhead.
- A complete first-order radio energy model is integrated to capture data transmission, reception, and aggregation, providing reasonable estimates of the node's energy consumption and enabling an accurate, fair comparison of different protocols.

1.3 Study Organization

The rest of this paper is structured as follows. Section 2 reviews existing clustering and routing methods, highlighting the research gap that this work addresses. Section 3 describes the methodology and presents the proposed QGE-K and other quantum-based routing protocols (FEQA, QE-PSCR). Section 4 simulation setup and describe the evaluation and performance analysis of our protocols in comparison with existing schemes. Section 5 describes the interpretation, aiming to highlight what our findings reveal. Section 6 describe the conclusion and possible direction of future studies.

2 Background Information and Related Work

2.1 Background Information

2.1.1 Wireless Sensor Network Model

WSNs consist of many low-cost, easily deployable sensor nodes that sense environmental factors such as temperature, humidity, light, and sound. These nodes are capable of self-organization, exchanging data within their communication range, and forwarding information in a multi-hop manner toward the base station [22]. In practical WSN deployments, communication reliability is affected by link-quality variations, interference, and packet loss. To approximate these effects, the first-order radio model is extended with distance-dependent path-loss adjustment and packet-success probability estimation. Transmission reliability is therefore modeled as a function of communication distance, where longer links lead to higher effective energy consumption due to potential retransmissions. Although the simulations assume homogeneous initial energy for clarity, the proposed clustering and routing framework supports heterogeneous energy configurations, since cluster-head selection already considers residual energy and neighbor density. Multi-hop interference is indirectly reflected through cumulative transmission cost and hop-count penalties in the routing evaluation. Detailed MAC-layer interference and stochastic packet-loss modeling are beyond the scope of this study and will be explored in future work targeting real-world deployments. The energy required to transmit (k) bits over distance (d) is explained in Eq. (1).

$$E_{Tx}(k,d) = \begin{cases} kE_{elec} + k\varepsilon_{fs}d^2, & d \le d_0 \\ kE_{elec} + k\varepsilon_{mp}d^4, & d > d_0 \end{cases} \tag{1}$$

where, E_{elec} is the electronic energy per bit, and $d_0 = \sqrt{\frac{\varepsilon_{fs}}{\varepsilon_{mp}}}$ is the threshold distance. The reception energy is given as in Eq. (2).

$$E_{Rx}(k) = kE_{elec} \tag{2}$$

and the energy for data aggregation is shown in Eq. (3).

$$E_{DA} = kE_{pub} \tag{3}$$

where (E_{pub}) is the aggregation cost per bit, and the parameter values are set according to widely used standards. To improve realism beyond the deterministic first-order radio model, an uncertainty-aware communication abstraction is introduced. Link reliability is modeled using packet reception probability based on the signal-to-interference-plus-noise ratio, enabling routing decisions to consider probabilistic packet loss under fading and interference. In dense networks, channel contention is reflected through an interference-aware adjustment factor in the routing fitness function. Although node mobility is not explicitly simulated, the framework supports periodic re-clustering and re-routing to adapt to topology changes, providing a more realistic representation of WSN deployment conditions. Table 1 containing symbols, parameters, and notation used in the system model, energy model, clustering formulation, and quantum optimization algorithms provides concise definitions of all important variables for improved Technical Transparency of Research

Table 1: Summary of used symbols and notations.

Symbol	Description
N	Total number of sensor nodes
K	Number of clusters
E_0	Initial energy of each node
$E_{Tx}(k, d)$	Energy consumed to transmit k bits over distance d
$E_{Rx}(k)$	Energy consumed to receive k bits
E_{DA}	Energy for data aggregation
E_{elec}	Electronic energy per bit
ε_{fs}	Free space amplifier energy
ε_{mp}	Multipath amplifier energy
d_0	Threshold distance for radio model
L_{net}	Network lifetime
FND, HND, LND	First, Half, and Last Node Death metrics
$mbest$	Mean best position in QPSO
$pBest$	Personal best particle position
$gBest$	Global best particle position
α_q	Contraction-expansion coefficient in QPSO
β	Lévy flight distribution parameter
μ	Logistic chaotic map control parameter
E_{RES}	Residual energy of node
E_{TOTAL}	Total network energy consumption

2.1.2 Cluster-Based Routing Protocol

Cluster-based routing protocols are essential, especially in WSN such as smart cities and IoT applications, and form the basis of efficient data collection and real-time monitoring [23]. The principle of operation for cluster-based routing is generally subdivided into CH selection, cluster formation, and data routing/transmission. In the CH selection stage, algorithms or target functions based on factors such as residual energy and distance to the BS determine which nodes become CHs. In the cluster-formation stage, nodes join the most suitable CH, typically based on proximity, thereby forming multiple clusters. In the routing stage, member nodes send data to their CHs via single-hop communication, while CHs forward data either directly to the BS or via multi-hop paths to conserve energy [24]. In LEACH, the threshold for CH selection is given by Eq. (4).

$$T(n) = \begin{cases} \dfrac{p}{1 - p \cdot (r \bmod (1/p))}, & n \in G \\ 0, & \text{otherwise} \end{cases} \tag{4}$$

where p is the desired proportion of CHs, r is the current round, and G is the set of nodes not selected as CHs in the past $(1/p)$ rounds. In large-scale networks, single-hop CH-to-BS communication results in excessive energy loss, so multi-hop cooperative transmission is preferred, where CHs forward data in steps toward the BS, thereby greatly improving scalability and energy efficiency.

2.1.3 Quantum Optimization Core Mechanism

This paper employs three quantum-inspired intelligent algorithms: the quantum genetic algorithm, the quantum annealing algorithm, and the quantum particle swarm algorithm, each relying on fundamental principles of quantum mechanics [25]. Quantum computing provides the foundation, where information is encoded in qubits that exist in a superposition of states, expressed as in Eq. (5).

$$|\varphi\rangle = \alpha|0\rangle + \beta|1\rangle, \quad \text{with } |\alpha|^2 + |\beta|^2 = 1 \tag{5}$$

Quantum logic gates such as Pauli (X, Y, Z), Hadamard, Phase (S), T, CNOT, and rotation gates enable reversible unitary transformations of qubits, ensuring stable manipulation of quantum states for optimization. For instance, the Hadamard gate creates superposition states, while rotation gates are commonly used to update solutions in quantum genetic algorithms, as in Eq. (6).

$$R(\theta) = \begin{bmatrix} \cos\theta & -\sin\theta \\ \sin\theta & \cos\theta \end{bmatrix} \tag{6}$$

The quantum adiabatic theorem provides the theoretical basis for quantum annealing. It states that if a Hamiltonian evolves slowly enough, the system remains in its ground state as shown in Eq. (7). The adiabatic condition as shown in Eq. (8) ensures transitions are avoided, enabling efficient convergence to optimal solutions.

$$H(t) = H_0 + V(t) \tag{7}$$

$$\frac{\langle \psi_i(t) | \frac{\partial H(t)}{\partial t} | \psi_j(t) \rangle}{(E_j(t) - E_i(t))^2} \ll 1 \tag{8}$$

Finally, the wave function $\psi(x,t)$ serves as a probability density amplitude and follows the Schrödinger equation, as shown in Eq. (9) which, when reformulated into imaginary time, resembles an iterative optimization process, is shown in Eq. (10).

$$i\hbar\frac{\partial\psi}{\partial t} = -\frac{\hbar^2}{2m}\frac{\partial^2\psi}{\partial x^2} + V\psi, \tag{9}$$

$$\frac{\partial\psi(x,t)}{\partial t} = D\frac{\partial^2\psi}{\partial x^2} - f(x)\psi(x,t). \tag{10}$$

In this study, different symbols are selected in order to facilitate unambiguous notations throughout, such as α denotes the quantum-state probability amplitude, α_q the QPSO contraction–expansion coefficient, α_p the proportional constant in assessing node potential, ω a fitness weighting coefficient and γ the annealing cooling or update factor. To ensure formal reproducibility, the quantum-inspired mechanisms used in this work are explicitly mapped to computational operators. In QGE-K, the quantum chromosome is represented as a probability amplitude vector, shown in Eq. (11).

$$|\psi\rangle = \alpha|0\rangle + \beta|1\rangle, \qquad |\alpha|^2 + |\beta|^2 = 1, \tag{11}$$

and updated using a quantum rotation gate as given in Eq. (12).

$$\begin{bmatrix}\alpha'\\ \beta'\end{bmatrix} = \begin{bmatrix}\cos(\Delta\theta) & -\sin(\Delta\theta)\\ \sin(\Delta\theta) & \cos(\Delta\theta)\end{bmatrix}\begin{bmatrix}\alpha\\ \beta\end{bmatrix}, \tag{12}$$

where the rotation angle $\Delta\theta$ is adaptively determined based on fitness comparison.

In FEQA, routing optimization is formulated as minimizing a Hamiltonian energy function, shown in Eq. (13).

$$H = \sum_i E_i + \sum_{i,j} w_{ij}x_ix_j, \tag{13}$$

where E_i represents node energy cost and w_{ij} denotes routing interaction weights. In QE-PSCR, particle positions follow a quantum delta potential well model, as expressed in Eq. (14).

$$x_i(t+1) = p_i(t) \pm \alpha_q|m(t) - x_i(t)|\ln\left(\frac{1}{u}\right), \tag{14}$$

where $u \sim U(0,1)$, $m(t)$ denotes the mean best position, and α_q is the contraction–expansion coefficient, consistent with Table 1. The Lévy flight perturbation is parameterized separately by a stability exponent λ, thereby avoiding ambiguity with the chaotic parameter u, shown in Eq. (15).

$$L(s) \sim |s|^{-1-\lambda}, \qquad 0 < \lambda \leq 2. \tag{15}$$

This is mathematically formalized quantum tunneling-like escape from local, optima-almighty optima. The formal definitions prove to be algorithmically reproducible and computationally verifiable.

2.2 Related Work

Wireless technologies are crucial for energy management in WSNs, especially since using energy category technologies optimally is necessary to exceed the lifetime of the network. WSNs are cost-effective for environmental, surveillance, and smart-city applications. Sensor nodes are not as battery-power-hungry, so

energy savings are highly prioritized until the cameras die inactive, where they are used to relay data in clear nodes performing multihop data transport. Many CH selection schemes unevenly use up energy that further decreases upon load at CHs, leading to network instability. The melding of communications with sensing and computing is paramount in vehicular ad hoc networks. Roadside Units are noted for their importance to data exchange and edge computing.

The study analyzes the literature according to its deployed techniques, reported advantages, and identified limitations to provide a clearer comparative understanding. Pandey and Hegde [26] propose a new approach that incorporates small-world characteristics to achieve low-latency, energy-balanced data transmission in WSNs. A cognitive small-world WSN adds new links between nodes and the sink, optimizing energy cost and leading to uniform energy consumption and faster, energy-efficient data transfer. Experimental simulations and the deployment of real nodes demonstrated that the approach increased the lifetime and improved energy efficiency and latency compared to previous protocols for medium- and large-scale applications. Witczak and Szymoniak [27] focus on monitoring and control of IoT systems. Different challenges were also analyzed. Some key technologies have been highlighted, and the use of data from different sources has also been discussed, which requires robust algorithms. Analyzing data will enhance the quality of IoT system usage. There are some cases of IoT applications in energy that illustrate the state of the art and stimulate research and technology in this area. Wang et al. [28] suggested a fused protocol that combines a fuzzy logic system with an FQA to improve network stability and reduce energy consumption. The FQA uses a fuzzy inference system to group CHs and employs the quantum annealing algorithm to route traffic from the CHs farthest from the base station in an optimal manner. Simulation results show that FQA outperforms competing methods across energy consumption, the number of alive nodes, network lifetime, and throughput in different scenarios. Similarly, chaos-PSO-based clustering methods improve convergence speed but may still face premature convergence in large-scale deployments. These observations highlight that although classical and intelligent metaheuristics enhance clustering performance, challenges related to convergence stability, computational overhead, and global optimization persist.

Chauhan et al. [29] proposed an improved CH selection method in which the K-means algorithm is used to ensure that the load is distributed evenly in the nodes in terms of energy. For CH selection, the Residual Energy parameter, the Nearby nodes, the Distance nodes from the Base Station, and the Signal Strength are considered. Simulation results show that the K-means-based CH selection method outperforms conventional protocols. Saxena and Singh Bhadauria [30] propose an energy-efficient routing protocol for hybrid WSNs with purposeful data aggregation, cluster-based routing and sleep scheduling specially designed for smart energy harvesting use. Their protocol is energy aware, uses sleep modes to save energy depending on node position and residual energy, and experimental results show it is better in terms of energy efficiency and lifetime rate than existing protocols. Tang and Nie [31] present a clustering-based SI routing algorithm for WSN using chaos particle swarm optimization to design a minimal-energy model, which finally generates energy-efficient clusters and selects cluster head nodes to aggregate data, thus extending the network's lifespan. It shows the experiment in which the stable time is improved for WSN by 30.10% over traditional algorithms, thereby lengthening the network's lifetime by 55.20%. Gu et al. [32] propose a network-based renormalization technique for RSU deployment that accounts for information flow and geographic locations. Compared to the optimal RSU deployment based on the evolutionary GA and memetic framework, the renormalization method exhibits better RSU coverage and information reception rates. Sattibabu et al. [33] propose a Federated Reinforcement Learning approach in which nodes share their experiences to create a single, continuously trained global model across sensor nodes. In simulation, a 13% improvement in packet delivery and a 15% improvement in energy efficiency over the DQN protocol.

A 30% improvement in packet delivery and a 24% improvement in energy efficiency over Reinforcement Learning-Based Routing have been achieved.

The comparative analysis in Table 2 reveals that existing WSN clustering and routing approaches still exhibit several research gaps. Many classical and metaheuristic methods face scalability issues and increased computational cost as the network size grows. They are also prone to premature convergence and local optima, especially in dense or dynamic environments. Moreover, most studies optimize clustering and routing separately, while parameter sensitivity under varying conditions remains a challenge. To address these issues, this study proposes three complementary quantum-inspired protocols. QGE-K improves clustering stability through quantum genetic optimization, FEQA combines fuzzy inference with quantum annealing for adaptive CH selection and energy-aware routing, and QE-PSCR jointly optimizes clustering and routing using quantum particle dynamics with chaotic initialization and Lévy flights. Together, these approaches enhance scalability, energy balance, and network.

Table 2: Summary of related works: algorithms, findings, advantages, and limitations.

Ref.	Algorithm/Technique	Key Findings	Advantages	Limitations
[34]	Glowworm Swarm Optimization + K-means	Improved coverage rate and clustering efficiency	Strong local search ability; enhanced coverage balance	High computational cost; scalability not validated
[35]	Quantum-Inspired Genetic Algorithm for fuzzy C-means initialization	Faster convergence and improved clustering center initialization	Better global search capability than classical GA	Deployed on clustering approach; not directly integrated into WSN routing
[36]	Quantum-Enhanced Grey Wolf Optimizer	Extended network lifetime and improved load balance	Effective global optimization; good stability in IIoT environments	Complexity increases with network scale; overhead in real-time systems
[37]	Optimal Fitness Distribution-based CH Update (Mobile WSN)	Improved CH rotation stability in mobility scenarios	Enhanced adaptability under node mobility	Less focus on static large-scale WSN scenarios
[38]	Quantum Clustering + K-means Hybrid	Improved cluster separation accuracy	Hybrid quantum-classical efficiency	Experimental; limited direct applicability to real WSN hardware
[39]	Optimal Relay Angle-based Clustering Routing	Reduced transmission energy via relay optimization	Efficient distance-based energy minimization	Focused only on relay angles; limited CH optimization
[40]	Ising Model + Annealing Methods	Improved theoretical stability modeling	Strong mathematical foundation	Limited large-scale WSN simulation validation
[41]	Improved PSO (Linearly Decreasing Inertia Weight)	Better clustering efficiency and energy balance	Faster convergence than standard PSO	Still prone to premature convergence

(Continued)

Table 2 (continued)

Ref.	Algorithm/Technique	Key Findings	Advantages	Limitations
[42]	Sine Cosine Algorithm + Lévy Mutation	Enhanced global search and routing efficiency	Improved exploration-exploitation balance	Increased computational overhead; limited large-network evaluation
[43]	Optimization-based Scheduling Algorithm	Improved scheduling efficiency	Strong task allocation optimization	Indirect application to WSN; not routing-specific

3 Proposed Methodology and Architecture

This study presents a framework for designing energy-efficient clustering and routing protocols in WSN using quantum-inspired optimization techniques. This architecture combines classical clustering techniques with other quantum computing concepts to achieve energy efficiency, network load balancing and network lifetime. The research methodology issues a network model and an energy model, and also describes multi-objective optimization functions for cluster head selection. Based on these models, three protocols were proposed: QGE-K, which uses quantum rotation gates; FEQA, which uses tunneling dynamics; and QE-PSCR, which uses probabilistic wave exploration. This architecture is used to define the hierarchy of the communication links among sensor nodes, cluster heads and base stations. Using fuzzy inference and quantum computation, dynamically optimize the node selection and routing.

3.1 Clustering Approach

The K-means algorithm is widely applied in clustering protocols for WSNs as a classic iterative clustering algorithm [38]. The core idea is to divide the N nodes within the detection range into K clusters, with each node assigned to the cluster whose centroid is closest to it, ensuring that the number of nodes in each cluster is as equal as possible. Through iteration, the sum of Euclidean distances from each node to its respective cluster centroid is minimized, as shown in Eq. (16).

$$\arg\min \sum_{i=1}^{n} \left\| x_i - a_j \right\|^2 \quad \text{where} \quad 1 \le j \le K \tag{16}$$

The label i_{label} is used to calculate the distance of all nodes in a cluster to the centroid node. When the sum of these distances is minimized, a cluster is formed, and the node closest to the cluster centroid is selected as the Cluster Head (CH). The Euclidean distance between nodes (x_i, y_i) and (x_j, y_j) is calculated using the Eq. (17).

$$d_{ij} = \sqrt{(x_i - x_j)^2 + (y_i - y_j)^2} \tag{17}$$

To enable adaptive determination of the optimal cluster number, the proposed QGE-K framework encodes the cluster count K directly into the quantum chromosome representation. Each chromosome contains a quantum bit string representing both cluster-head selection and candidate cluster-number configurations. The probability amplitudes of the quantum bits are updated using rotation gates based on

fitness comparison between current and global best solutions. The fitness function guiding adaptation is defined as a multi-objective function, shown in Eq. (18).

$$F = w_1 \cdot \frac{1}{\sigma_E} + w_2 \cdot \frac{D_{\text{inter}}}{D_{\text{intra}}} + w_3 \cdot \frac{1}{L}, \tag{18}$$

where σ_E denotes the variance of residual energy among cluster heads, D_{intra} represents the average intra-cluster distance, D_{inter} denotes inter-cluster separation, L represents the estimated network lifetime, and w_1, w_2, w_3 are weighting coefficients. During evolution, candidate values of K are evaluated according to this fitness function. The rotation angle $\Delta\theta$ decreases progressively as fitness improvement diminishes, ensuring stabilization. Convergence is considered achieved when the condition in Eq. (19) is satisfied.

$$|F(t) - F(t-1)| < \varepsilon, \tag{19}$$

where ε is a predefined small threshold.

The K-means algorithm is a simple, efficient, and easy-to-implement method, known for its fast execution. However, in large networks with uneven node distribution and non-spherical deployment, the random selection of initial centroids significantly affects clustering results. To address these two issues, we optimize the algorithm by determining the optimal number of clusters and using a quantum genetic algorithm to select the most suitable initial CHs, thereby reducing the K-means algorithm's iteration time. Karpurasundharapondian and Selvi [44] propose a cluster routing protocol based on Cuckoo Search optimized K-means. The protocol uses the Cuckoo search algorithm to elect reasonable initial CHs, improving K-means' insensitivity to initial cluster centers. Gunjan et al. [45] propose a non-uniform cluster-based routing protocol in which the clustering and routing problem is solved using the Genetic Algorithm.

3.2 Routing Scope and Path

If all the Cluster Heads directly transmit data to the BS, the CHs located farther from the BS would consume excessive energy and die prematurely. To reduce communication overhead and optimize data transmission paths, this protocol adopts a multi-hop routing approach, which allows data to be forwarded through multiple intermediate CHs until it reaches the BS. In large-scale network scenarios, multi-hop routing can achieve load balancing and extend the network lifetime. This paper further constrains the planning of the optimal routing path by defining the selection range for the next-hop node. The first consideration is to find the next-hop node between the current CH i_{CH} and the BS. That is, the distance between the i_{CH} and the next-hop node should be smaller than the distance between the current CH i_{CH} and the BS. Therefore, we define the radius as the distance from the i_{CH} to the BS, which is calculated using Eq. (20).

$$r_{\text{iCH-BS}} = \sqrt{(x_{\text{iCH}} - x_{\text{BS}})^2 + (y_{\text{iCH}} - y_{\text{BS}})^2} \tag{20}$$

where $(x_{\text{iCH}}, y_{\text{iCH}})$ is the coordinates of the current cluster head i_{CH}, and $(x_{\text{BS}}, y_{\text{BS}})$ are the coordinates of the base station. Then, two arcs are drawn with centers at i_{CH} and BS, and radii r_1 and r_2. We connect i_{CH} with r_1 and r_2 and extend them to define the selection range for the next-hop node. After satisfying the above conditions, the proposed protocol designs a fitness function considering energy, distance, and load to select the next-hop node. If the distance from all potential next-hop nodes within the range to i_{CH} is greater than the distance to the BS, the current CH i_{CH} directly transmits data to the BS. The fitness function is given by Eq. (21).

$$f(CH_{i+1}) = \eta_1 \left(\frac{E_{\text{initial}}}{E_{\text{RES}}} \right) + \eta_2 \left(d_{\text{CH}_i,\text{CH}_{i+1}} \right) + \eta_3 \left(\text{load}(CH_{i+1}) \right) \tag{21}$$

where E_{initial} is the initial energy of the node, E_{RES} is the current remaining energy of the node, $d_{\text{iCH},i+1}$ is the distance from the cluster head i_{CH} to the next-hop cluster head $i_{\text{CH}+1}$, and $\text{load}_{i_{\text{CH}+1}}$ is the load of the next-hop cluster head. To minimize energy consumption and extend the network lifetime, the next-hop node with the highest remaining energy, the shortest distance, and the lowest load should be selected, i.e., the CH with the smallest fitness function value.

3.3 Cluster Head Selection Based on Fuzzy Logic

In the Fuzzy Logic-Based Selection stage, the Fuzzy Inference System calculates the probability that each node in S_{CH} becomes a CH based on its remaining energy, $E(N)$. As CHs are key for data transmission and consume significant energy, the FQA protocol sets an energy threshold. Select the nodes with the most substantial remaining energy as candidate CHs and have input parameters.

1. **Residual Energy ($f_{1\text{CH}}$):** It presents the residual energy of node i in the current round, denoted as $E(i)$. CHs are crucial nodes for data transmission and consume significant energy. As the network runs, this parameter becomes increasingly critical.
2. **Number of Neighboring Nodes ($f_{2\text{CH}}$):** It represents the number of one-hop communication connections every node establishes with the surrounding nodes within its communication range, reflecting the compactness of the cluster. The larger this parameter's value, the shorter the distance between nodes in the cluster.
3. **Distance to BS ($f_{3\text{CH}}$):** It is the Euclidean distance from the candidate node i and BS, denoted as $\text{Dis}(i, \text{BS})$. Nodes nearer to the BS are chosen more frequently as CHs, since they use less energy for communication. As nodes remain static, during the initial iteration, the BS gathers distance data from all nodes using the Received Signal Strength Indicator.
4. **Node Centrality ($f_{4\text{CH}}$):** In this protocol, CHs are selected before the cluster formation. Therefore, we define the node centrality as the average distance between candidate CHs and their neighboring node set ($\text{Neighbor}(i)$), calculated using Eq. (22).

$$f_{4\text{CH}}(i) = \frac{1}{|\text{Neighbor}(i)|} \sum_{j \in \text{Neighbor}(i)} d(\text{CH}_i, j) \tag{22}$$

where $d(\text{CH}_i, j)$ is the Euclidean distance between the candidate CH i and its neighboring node j. A smaller value of $f_{4\text{CH}}$ indicates that the candidate CH is closer to the center of the cluster. Selecting nodes closer to the cluster's centroid minimizes the total energy required for data transmission within the cluster.

Where $d(\text{CH}_i, j)$ is the Euclidean distance between the candidate CH i and its neighboring node j. The smaller the value of $f_{4\text{CH}}$, the closer the candidate CH is to the center of the cluster. Selecting nodes closer to the cluster's centroid helps minimize the total energy required for data transmission within the cluster. Using the above input variables, the FIS outputs a likelihood value indicating the likelihood that a node will become a CH. Fig. 1 depicts the entire process, which includes normalization, fuzzification, fuzzy logic system, and defuzzification.

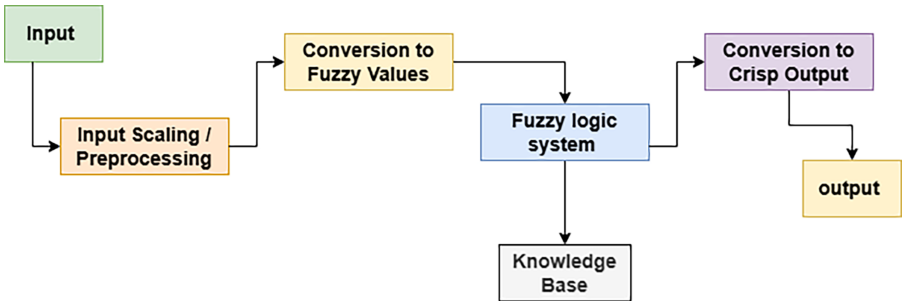

Figure 1: The FIS of the FEQA protocol demonstrating the process of cluster head selection based on input parameters such as residual energy, node centrality, distance to base station, and neighboring node density.

The purpose of normalization is to transform input variables with diverse magnitudes into a standard range of 0 to 1. This step transforms the membership values to a standard scale, making them easier to compare and calculate. Every normalized variable is assigned to the relevant fuzzy linguistic parameter through a membership function. In the proposed study, every selected input variable in the fuzzy system has a distinct membership function. FQA uses trapezoidal and triangular membership functions. The linguistic variables design all FISs, and the fuzzy output is obtained from the feature set selected by the optimization process. After CH selection, each CH broadcasts its message within its communication range. Each node then associates with the CH having the highest potential value.

$$p_N = \frac{\alpha_p E_{\text{ch}}(i)}{N \cdot \text{Dis}(S, CH)} \tag{23}$$

In Eq. (23), p_N represents the potential value of the node, $E_{\text{ch}}(i)$ is the remaining energy of the selected CH, and $\text{Dis}(S, CH)$ is the Euclidean distance between the CH i_{CH} and the member node j_S. The constant α_p is a proportional constant. Since nodes with higher remaining energy were selected as candidate CHs in Section 4.2, we treat the $\text{Dis}(S, CH)$ as a more critical factor. Based on simulation comparisons, we set $\alpha_p = 0.3$. Chauhan et al. [29] presented a fuzzy logic-based relay node selection and energy-efficient routing protocol. Based on FIS, node selection considers coverage distance, remaining energy, efficiency factor, and bandwidth availability as input variables.

3.4 Quantum Particle Swarm Algorithm

In this paper, we introduce a new algorithm for searching optimal clustering results based on Quantum Particle Swarm Optimization (QPSO). This novel optimization method combines the characteristics of classical PSO with properties of quantum mechanics. QPSO extends the basic PSO by eliminating the velocity term and using the space dimensions of quantum mechanics. In QPSO, the particles do not have velocity vectors, as in traditional PSO; instead, their positions are updated using a quantum-inspired method that provides a contraction-expansion process. The algorithm works by evaluating the fitness of each particle's position in the swarm and, at each iteration, determining whether the particle's current position is better than its own best known position and the swarm's best known position. Thus, if a particle's present position gives better fitness, it becomes recorded as its best known position. The global best position is also updated if any particle is found to have a better fitness than the previous global best. The process is repeated iteratively until some resting criterion is met, such as a predetermined number of iterations or convergence to the extent that a solution exists. The quantum particle swarm optimization approach provides an effective search for solutions to clustering and routing, as well as other optimization problems, where it excels by allowing greater

exploration of the search space without the need for specific velocity components. This approach provides a suitable alternative to classical optimization techniques in machine learning problems. The weight factor is calculated as Eq. (24).

$$w = w_{\max} - \frac{(w_{\max} - w_{\min})}{\max} \tag{24}$$

Among them, $x_{\min} \in [0,1]$. The fitness function is expressed as in Eq. (25).

$$f = \omega E(CH) + (1-\omega) \times \mathrm{dis}(n, CH) + \mathrm{dis}(CH, BS) \tag{25}$$

In the formula, the first term considers the remaining energy of the node, and the latter terms consider the distances from the node to CH and from CH to BS. For cluster n, when CM is selected, the cluster is based on the weight factor of each CH as shown in Eq. (26).

$$W_{CH}(s, CH) = \frac{E(CH)}{\mathrm{dis}(s, CH) \times \mathrm{dis}(CH, BS) \times \mathrm{node\_degree}(CH)} \tag{26}$$

The CH transmits data to neighboring CHs using the minimum energy routing protocol until it reaches the BS. When the distance between CH and BS is less than a threshold, data is directly single-hopped to BS.

Hu and Tong [46] proposed a self-adaptive PSO algorithm and non-uniform routing protocol (APSO-NUCR) as shown in Eq. (27).

$$T(i) = \begin{cases} E(i) - E_{ave}, & E(i) \geq E_{ave} \\ 0, & E(i) \leq E_{ave} \end{cases} \tag{27}$$

The distance factor is given by Eq. (28).

$$R = 1 - c\frac{d_{\max} - d(i, \mathrm{Sink})}{d_{\max} - d_{\min}} \tag{28}$$

Here, $d_{\max}$ and $d_{\min}$ denote the maximum and minimum node-to-node distances, respectively. The learning factor in APSO-NUCR is self-adaptive, enhancing convergence toward optimal positions. The routing phase uses the Prim algorithm to construct a minimum spanning tree.

3.5 Multi-Hop Routing Strategy

Metropolis, inspired by the annealing technique in physics, emulated the metal-smelting annealing process and introduced the Simulated Annealing (SA) algorithm. This algorithm utilizes the Monte Carlo Markov chain method of statistical mechanics to identify the optimal solution that minimizes the objective function among various candidate solutions [47]. Whereas the SA algorithm jumps over obstacles to escape local minima, the Quantum Annealing algorithm (QA) adds a tunneling part to the quantum algorithm to develop quantum fluctuations that allow the system to tunnel through potential barriers to the lowest energy configuration, a phenomenon known as quantum tunneling. Like SA, the QA algorithm cools its way down through a process from high to low temperatures. With the kinetic energy term important, and thus closer to that of quantum tunneling, it traverses the whole solution space in the early stages of annealing. The kinetic energy term will decrease towards zero at later times, clearly leading the system to evolve from a predominantly quantum-mechanical state to one that is more evidently classical. The development of a

quantum system, influenced by both potential and kinetic energy, is articulated through the Schrödinger equation as shown in Eq. (29).

$$i\hbar\frac{\partial}{\partial t}\Psi(r,t) = \hat{H}(r,t)\Psi(r,t) \tag{29}$$

where $\Psi(r,t)$ is the wave function that describes the state of a quantum system; $\hbar$ is Planck's constant; $\hat{H}$ is the Hamiltonian operator, representing the total energy of the system, which is given in Eq. (30).

$$\hat{H} = -\frac{\hbar^2}{2m}\nabla^2 + V(r) \tag{30}$$

where m is the mass of the particle, ∇ is the gradient operator, and $V(r)$ is the potential field of the particle. In practical applications, the complexity grows exponentially with the problem's complexity.

This paper uses the Path Integral Monte Carlo approach to model the quantum annealing process, facilitating the transition from classical to quantum dynamics. The PIMC process is elucidated using a two-dimensional random Ising model. Each arrow $a_i \in \{-1, +1\}$ symbolizes a small magnetic dipole with varying spin orientations, and the collective spin directions of these dipoles dictate the system's overall magnetization. The interactions between neighboring dipoles and the thermal noise of the environment influence the direction of each dipole. As the temperature increases, thermal noise interference becomes more pronounced, and the combined effect of these interactions disordered the magnetization within the dipoles. However, during annealing, as the temperature gradually decreases, the dipole-dipole interactions become more pronounced. When the temperature is sufficiently low, the magnetization of most dipoles aligns, and the system reaches its lowest energy state. Based on the transverse magnetic field Ising model, the optimization problem's objective function minimization can be converted into the quantum ground state's Hamiltonian (potential energy), expressed as Eq. (31).

$$H_p(t) = \sum_{i=1}^{N} h\sigma_i^z + \sum_{i,j=1}^{N} J_{ij}\sigma_i^z\sigma_j^z \tag{31}$$

In this paper, h_i denotes the external local longitudinal magnetic field, which is assumed to be zero for simplicity; J_{ij} indicates the coupling strength between quantum bits i and j; σ_i and σ_j are the Pauli Z operators located at sites i and j, respectively. From the Ising model's Hamiltonian, we can derive the Hamiltonian for the QA algorithm.

$$H(t) = H_p(t) + \Gamma(t)\sum_{i,j=1}^{N}\Delta_{ij}\sigma_i^x \tag{32}$$

In Eq. (32), Γ is the field strength, which induces the up and down transitions of the single quantum bit's spin states, similar to the temperature T in the SA algorithm.

3.6 Proposed Clustering Routing Protocol Based on Quantum Genetic-Enhanced K-Means (QGE-K)

The QGA-K protocol involves two processes: clustering and routing. Therefore, its time complexity is represented as $O(\text{QGA-K}) = O(\text{Clustering Time Complexity} + \text{Routing Time Complexity})$. First, solving for the optimal number of clusters K requires only a single formula derivation, so the time complexity is $O(1)$. When calculating the optimal initial cluster heads, the population size is M, and the total number of alive nodes is N. The time complexity of the population initialization phase is $O(M \times K)$; the time complexity of the fitness function calculation is $O(M \times N \times K)$; the time complexity of the quantum rotation gate

update is $O(M \times K \times L)$, where L is the quantum bit encoding length, and $L = N$, so the time complexity of the quantum rotation gate update is $O(M \times K \times N)$. The time complexity of the K-means algorithm for clustering is $O(K \times N^2)$. In the routing phase, each cluster head evaluates candidate next-hop cluster heads within the constraint range. In the worst-case scenario (i.e., a fully connected network), the calculation is done for all cluster heads. The time complexity in this phase is $O(K^2)$. Therefore, the total time complexity of the QGA-K protocol is ultimately $O(K \times N^2)$. Algorithm 1 outlines the QGE-K approach, which combines quantum genetic optimization with K-means clustering. This method tackles these challenges successfully and results in more balanced and energy-efficient cluster formation.

Algorithm 1: Optimized clustering with quantum genetic algorithm

Input: Sensor node positions, residual energy, and communication range
Output: Energy-efficient clusters and optimized routing paths
Initialization: Set nodes in the network, BS position and communication range;
Compute optimal cluster count K based on network size and average node-to-BS distance;
Step 1: Quantum Genetic Initialization;
for *each node i* **do**
    Encode node as a quantum chromosome: $Q_c = [a_1, a_2, \ldots, a_N]$, where $a_i = 1$ indicates a candidate CH;
Initialize population of M chromosomes Q_p;
for *each chromosome* Q_p **do**
    Repeat Steps 7–9 for $t = 1, \ldots, G_{\max}$ or until $\left|f^t best - f^{t-1} best\right| < \epsilon$, where $G_{\max}$ is the maximum generation number and ϵ is the convergence tolerance.
    Evaluate fitness:
    $fit(i) = \alpha E_{\mathrm{RES}}(i) + \beta \mathrm{Neigh}(i)$
    Update chromosomes using a quantum rotation gate:
    $R(\theta) = \begin{bmatrix} \cos\theta & -\sin\theta \\ \sin\theta & \cos\theta \end{bmatrix}$
    Adjust $\Delta\theta$ and rotation direction *s(a,m)* according to convergence behavior;
    Apply the quantum NOT gate to maintain population diversity;
Select K optimal CHs with maximum fitness;
Step 2: K-means Clustering;
for *each CH* CH_i **do**
    Use selected CHs as initial centroids;
    for *each node j* **do**
        Assign node *j* to the nearest CH based on Euclidean distance;
    Iteratively update centroids until convergence;
Step 3: Routing Optimization;
for *each CH* CH_i **do**
    Compute the distance between each CH and BS:
    $r = \sqrt{(x_{\mathrm{CH}} - x_{\mathrm{BS}})^2 + (y_{\mathrm{CH}} - y_{\mathrm{BS}})^2}$
    Construct multi-hop routing paths within defined sector regions;
    for *each node in the sector* **do**
        Select next-hop CH using residual energy, inter-CH distance, and CH load criteria;
        Transmit data from CHs to BS via optimized routes;
    Update node energy and re-cluster if CH energy < $E_{\mathrm{threshold}}$;
return *Optimized clusters and routing minimizing total energy consumption;*

3.7 Proposed Clustering Routing Protocol Based on Fuzzy-Enhanced Quantum Annealing Algorithm (FEQA)

This research proposes a FEQA routing protocol based on fuzzy logic and the quantum retreat algorithm. FEQA protocol helps find the most efficient energy route (CH to BS). An effective data transmission mode has been established using a fuzzy-logic segmentation model and a quantum retreat-based routing algorithm, thereby increasing the network lifespan. Using the energy threshold, nodes are screened to reject redundant CH submissions and identify optimal CHs. The selection is through the Fuzzy Inference system, which takes four parameters as fuzzy input variables, namely, remaining energy, neighboring node number, distance to base station, and node centrality. Finally, the optimal routing scheme is determined by evaluating the objective function and transforming the result into a quantum state.

The time complexity of the FQA protocol can be expressed as the sum of three main computational stages: candidate cluster-head selection, fuzzy inference processing for optimal cluster-head determination, and the quantum annealing optimization used for routing path selection. Therefore, the overall time complexity of the FQA protocol can be written as $O(\text{FQA}) = O(\text{Candidate Cluster Head Selection}) + O(\text{FIS for Optimal CH Selection}) + O(\text{Quantum Annealing for Optimal Path})$, where each term represents the computational cost associated with the respective stage of the protocol. To filter candidate cluster heads, we need to traverse all nodes' energy thresholds, so the time complexity is $O(N)$. The degree of membership for each candidate node is calculated for the four input variables. Based on 135 fuzzy rules, the K CH are evaluated from the CHS, and the time complexity for this process is $O(S_{\text{CH}} + 135 \times S_{\text{CH}})$. The total complexity of the clustering time is $O(N)$. In the routing phase, we need to construct $O(K^2)$ coupling terms to represent communication energy, and the Hamiltonian construction complexity is $O(K^2)$. The time complexity of decoding the optimal path is $O(K)$. Therefore, the total complexity of the routing time is $O(K^2)$. Since $K \leq N$, the overall time complexity of the FQA protocol is $O(N + K^2)$. The routing planning process is shown in Algorithm 2.

Algorithm 2: Quantum annealing algorithm: route planning implementation

Input: Initial parameters: M, $L_{best} = L^0$, $\Gamma = \Gamma^0$, $M_e = Maxsteps$, $k = 0$
Output: Optimized route plan L_{best}
while $\Gamma > \Gamma_{\min}$ **and** $M_e > 0$ **do**
  Compute quantum coupling coefficient:
  $J_r = -\frac{T}{2\ln\tan\left(\frac{\Gamma}{T_1}\right)}$
  while $k < n$ **do**
    Generate a new candidate route:
    $L^k = O\{L^t\}$
    Compute energy differences:
    $\Delta H_p = H_p(L^t) - H_p(L^k)$
    $\Delta H_k = H_k(L^t) - H_k(L^k)$
    $\Delta H_c = \frac{\Delta H_p}{n} - J_r \Delta H_k$
    if $\Delta H_p \leq 0$ **then**
      $L^t = L^k$
    if $H_p(L^k) \leq H_p(L_{best})$ **then**
      $L_{best} = L^k$
    else if $\Delta H_k \leq 0$ **then**

(Continued)

Algorithm 2 (continued)

$L^t = L^k$
else if $\exp(-\Delta H_c/T) > random(0,1)$ **then**
$L^t = L^k$
Increment the iteration counter: $k = k + 1$;
Update temperature and annealing parameters:
$T = T \times \gamma_T, \quad \Gamma = \Gamma \times \gamma_\Gamma$
$k = 0$; Decrease iteration counter: $M_e = M_e - 1$;
return L_{best}

Here, `Maxsteps` refers to the maximum number of Monte Carlo steps; L' represents the candidate solution, and the operator O is used to update the current solution.

3.8 Proposed Clustering Routing Protocol Based on Quantum-Enhanced Particle Swarm Clustering and Routing (QE-PSCR)

A cluster routing protocol based on an intelligent optimization algorithm is one of the most effective methods to achieve energy balance in WSNs. However, due to its inherent disadvantages, such as time consumption, limited species diversity, and a tendency to fall into local optimization, its performance is unstable. This research presents a cluster routing protocol based on a QE-PSCR. Compared to the standard QPSO algorithm, this algorithm introduces particles into the quantum space, where each particle is described by a wave function. Compared with the standard particle swarm optimization algorithm, it reduces the number of control parameters and eliminates the influence of the speed limit. In addition, the algorithm utilizes the Logistic sequence to initialize the particles, thereby achieving diversity among them. Algorithm 3 provides an overview of the proposed QE-PSCR approach, which integrates quantum-enhanced particle swarm optimization with chaotic mapping and Lévy flight strategies to achieve balanced clustering and energy-efficient routing.

Algorithm 3: QE-PSCR–quantum-enhanced particle swarm clustering and routing protocol

Input: Network parameters, node energy model, $Iter_{max}$, chaotic factor μ, coefficient α_q, convergence tolerance ϵ
Output: Optimized clusters and routing paths minimizing E_{TOTAL}
Initialization: Initialize particle positions Q_i, velocities, α, μ, and $E_{TOTAL} = 0$;
Set $pBest_i = Q_i$, $gBest = \arg\min f(pBest_i)$;
Set iteration counter $t = 0$;
Step 1: Chaotic Initialization;
Generate each $q_{t+1,i} = \mu q_{t,i}(1 - q_{t,i})$, where $3.57 \le \mu \le 4$;
Step 2: Fitness Evaluation;
$f = \beta E_{NET} + (1-\beta)E_{dev}$, with $E_{NET} = \sum E_{CLS_k}$ and $E_{dev} = \sqrt{\frac{1}{m}\sum(E_{CLS} - E_{AVG})^2}$;
Step 3: Iterative Optimization;
while $t < Iter_{max}$ **and** $|f(gBest^t) - f(gBest^{t-1})| > \epsilon$ **do**
Compute $m_{best}(t) = \frac{1}{N}\sum pBest_i(t)$;
Update positions: $Q_i^{t+1} = p_i^t \pm \alpha_q |m_{best}(t) - Q_i^t| \ln(1/u_i), \qquad u_i \sim U(0,1)$
Apply Lévy flight: $Q_i^{t+1} = Q_i^{t+1} + \frac{\mu}{|v|^{1/\beta}}, \ \beta = 1.5$;
Apply Lévy-flight perturbation: $Q_i^{t+1} = Q_i^{t+1} + s_i, \qquad s_i \sim Levy(\lambda), \ \lambda = 1.5$

(Continued)

Algorithm 3 (continued)

Re-evaluate fitness, update $pBest_i$, $gBest$;
Compute $E_{CH} = (r + m)E_{TX}(d) + (r + 1)E_{RX}(d) + E_{DA}$;
$E_{TOTAL} \leftarrow E_{TOTAL} + E_{CH}$;
if $d(CH, BS) < d_{th}$ **then**
    Direct transmission;
else
    Multi-hop via CH with max E_{RES};
$t = t + 1$;
Update total energy: $E_{TX} = \sum |gBest|^2 + E_{TX}$; $E_{TOTAL} += E_{TX}$;
Compute routing energy E_{route} based on optimized paths and update:
$E_{TOTAL} \leftarrow E_{TOTAL} + E_{route}$
return Optimized clustering and routing minimizing E_{TOTAL};

The Lévy flight is selected to update the particles, thereby preventing them from falling into local optima. Both the QPSO contraction–expansion coefficient $\alpha_{q'}$, the μ parameter reserved exclusively for chaotic logistic initialization and the α Lévy-flight stability exponent have been used consistently throughout the QE-PSCR. All cluster-head communication costs at each iteration have been added to the route-transmission cost for the total-energy update. QPSO is compared with the latest Black Widow Optimization Algorithm (BWO) and Dung Beetle Optimizer (DBO). The improved QPSO (IQPSO) exhibits enhanced global search capabilities and higher accuracy.

In QE-PSCR, the optimal number of clusters, the best-balanced cluster, and the routing path are computed. A new fitness function is set to evaluate the particle quality. To avoid calculation overload, an on-demand maintenance scheme is used. In simulation, they study existing protocols' performance, with LDIWPSO and APSO-NUCR, in terms of power consumption, throughput, and lifetime of the network. In all cases, QE-PSCR performs well. After deploying the sensor network, remaining energy, etc. Once the BS gathers all the info, it executes the QE-PSCR protocol. Determining the CHs and forming clusters is already done, and searching for the routing path by encoding it all in one particle to optimize this process. Selecting candidate CHs, setting up the initial population, defining a fitness function, and updating the position are all performed. To reduce energy consumption and ensure load balance, a single, on-demand maintenance mechanism is employed. Data needs to be collected and loaded into BS to ensure energy consumption is accounted for, so that clusters that are nearer to them shall die faster as they consume energy more quickly. So it follows suit that its maintenance is needed to extend the network lifetime. In their protocol, it simply stops when the owner node dies. The QE-PSCR protocol determines the best cluster, performs cluster formation, and searches for the routing code on a single particle. To make the joint encoding explicit, QE-PSCR treats each particle as a composite representation of clustering decisions and routing decisions among the selected cluster heads. Hence, the search-space dimensionality increases with network size because both node-level and cluster-head-level variables are optimized simultaneously. If n denotes the number of sensor nodes and m denotes the final number of cluster heads, then the particle dimension grows with the clustering component $O(n)$ plus the routing component among cluster heads $O(m^2)$, yielding an overall scaling on the order of $O(n + m^2)$. Because the combined search space is highly constrained, QE-PSCR uses three feasibility mechanisms during optimization: repair rules to correct invalid cluster assignments, such as reassignment to the nearest valid cluster head; a penalty-augmented fitness evaluation that discourages infeasible routing structures or energy-violating solutions; and routing pruning and validation that remove disconnected links and resolve loops before fitness acceptance. This ensures that

the single-particle encoding does not result in uncontrolled infeasible exploration. Finally, to make scalability explicit, the per-iteration computational cost is dominated by evaluating the clustering and routing fitness terms and validating feasibility, which aligns with the manuscript's existing time-complexity statement. The time complexity for initialization is $O(n^2)$, and the time complexity of the evaluation function is $O(n^2 + n^2 \times m)$. The update operation has a time complexity of $O(m)$, where m represents the final number of cluster heads in the cluster routing coding scheme.

4 Experiments Analysis

To evaluate the performance and effectiveness of the proposed quantum optimization-based clustering and routing protocols, such as QGE-K, FEQA, and QE-PSCR, comprehensive simulation experiments were conducted. This study performs simulations that consider lifetime, energy consumption, and capacity increase for different scheme sizes and densities, then compares the protocols against SATA algorithms, showing they achieve marked improvements in load balance and routing stability. Longer network lifetime, less energy consumed, and more reliable in transmitting messages than classical and traditional intelligent optimization protocols.

4.1 Evaluation Parameters

This investigation assesses performance within the framework of conventional, widely accepted parameters for a WSN's energy efficiency, stability, reliability, and scalability. A widely accepted definition of network lifetime is the duration from the start of network operation until the last sensor node dies. This is a key parameter used to assess energy efficiency and sustainability of a WSN. The proposed study is generally considered to have a three-phase lifespan.

- First Node Death (FND): The round in which the first node dies.
- Half Node Death (HND): Around 50% of the nodes die.
- Last Node Death (LND): The round in which the last node dies and the network's useful life ends.

Mathematically, the network lifetime L_{net} can be expressed as in Eq. (33).

$$L_{\text{net}} = R_{\text{LND}} - R_{\text{FND}} \tag{33}$$

where R_{FND} and R_{LND} denote the rounds of initial and final node death, respectively.

Energy consumption is the measure of total energy consumed by each node during transmission, reception, and data aggregation, illustrated in Eq. (34).

$$E_{\text{consumed}}(r) = \sum_{i=1}^{N} \left(E_i^{\text{initial}} - E_i^{\text{residual}}(r) \right) \tag{34}$$

where E_i^{initial} is the initial energy of node i, and $E_i^{\text{residual}}(r)$ is its residual energy after round r.

The PDR measures the reliability of data transmission from the sensor nodes to the base station, as defined in Eq. (35).

$$PDR = \frac{P_{\text{received}}}{P_{\text{sent}}} \times 100 \tag{35}$$

where P_{received} and P_{sent} represent the number of successfully received and transmitted packets, respectively.

The alive nodes per round parameter tracks the number of sensor nodes still active in each round, i.e., those with $E_i > 0$. It is used to assess network stability and energy balancing across the simulation timeline.

$$N_{\text{alive}}(r) = \sum_{i=1}^{N} \delta(E_i^{\text{residual}}(r) > 0) \tag{36}$$

where in Eq. (36), $\delta(\cdot)$ is an indicator function equal to 1 if the node is alive and 0 otherwise.

The End-to-end delay represents the average time it takes for data packets to reach the Base Station from source nodes, including transmission, propagation, and processing delays.

$$D_{\text{avg}} = \frac{\sum_{i=1}^{P_{\text{received}}} (t_i^{\text{recv}} - t_i^{\text{send}})}{P_{\text{received}}} \tag{37}$$

where in Eq. (37) t_i^{send} and t_i^{recv} denote the sending and receiving times of the ith packet.

Load balancing ensures even energy consumption among nodes, especially CHs. The load balancing factor (LBF) can be expressed as in Eq. (38).

$$LBF = \sqrt{\frac{1}{N} \sum_{i=1}^{N} (E_i^{\text{residual}} - \bar{E})^2} \tag{38}$$

where $\bar{E}$ is the average residual energy of all nodes. A smaller LBF indicates better energy balance across the network.

Convergence speed measures how quickly an optimization algorithm converges to a stable or near-optimal solution. It is generally defined as the number of iterations required for convergence.

$$t_{\text{conv}} = \min(t) \text{ such that } |F(t) - F(t-1)| < \epsilon \tag{39}$$

where in Eq. (39) $F(t)$ is the fitness value at iteration t, and ϵ is a small convergence threshold.

The stability period defines the time interval between network initialization and the death of the first node. It represents the most reliable and energy-efficient operation phase of the network, as shown in Eq. (40).

$$S_{\text{period}} = R_{\text{FND}} \tag{40}$$

4.2 Experimental Setup

The performance of the proposed quantum optimization-based clustering and routing protocols, including QGE-K, FEQA, and QE-PSCR, was evaluated through simulations. To avoid ambiguity across the three experimental subsections, we adopt a globally unique scenario-labeling convention throughout the study. Specifically, scenarios used in the QGE-K evaluation are denoted as QGE-S1 and QGE-S2; scenarios used in the FEQA evaluation are denoted as FEQA-S1 to FEQA-S4; and scenarios used in the QE-PSCR evaluation are denoted as QPSCR-S1 to QPSCR-S4. The nodes were randomly deployed, homogeneous, and stationary with an initial energy of 0.5 J. The classical first-order radio energy model was used, and communication followed single-hop and multi-hop schemes depending on the CH-BS distance. Each simulation was run for up to 1600 rounds, and the results were averaged over multiple runs to ensure statistical consistency. The proposed protocols were compared with benchmark algorithms, including CS-K, GA-UCR, FRNSEER, and APSO-NUCR, using identical configurations. The parameter values are listed in Table 3. The simulation parameters are commonly adopted for the first-order radio energy model used in

wireless sensor network studies. In this model, the electronic energy E_{elec} represents the energy consumed by the transmitter or receiver circuitry, while ε_{fs} and ε_{mp} represent the free-space and multipath channel amplification parameters, respectively. The packet size of 4000 bits and the initial node energy of 0.5 J are widely used benchmark values in WSN clustering experiments. Two network areas (100×100 m^2 and 400×400 m^2) with node populations of 100 and 200 are considered to evaluate the scalability of the proposed protocol under both moderate and larger deployment conditions.

Table 3: Simulation parameters.

Parameter	Symbol/Unit	Value
Initial Energy per Node	E_0	0.5 J
Electronic Energy	E_{elec}	50 nJ/bit
Data Aggregation Energy	E_{DA}	5 nJ/bit
Free Space Amplifier	ε_{fs}	10 pJ/bit/m^2
Multipath Amplifier	ε_{mp}	0.00014 pJ/bit/m^4
Threshold Distance	d_0	$\sqrt{\varepsilon_{\text{fs}}/\varepsilon_{\text{mp}}}$
Packet Size	k	4000 bits
Simulation Rounds	r	0–1600

4.3 Performance Evaluation of the QGE-K Based Clustering Routing Protocol

Experiments were conducted on the QGE-K protocol and compared with existing protocols, including CS-K [44], GA-UCR [45], FQA [28], GEGWO-CR [48], BOA-QCR [28], and QGA [49] in various scenarios. The protocol's performance was evaluated using several indicators, including network lifetime, power consumption, and throughput. Two network scenarios were considered to evaluate scalability. These scenario definitions are consistently used throughout the study. The simulation was conducted in an area of 100 m × 100 m and a large-scale network of 400 m × 400 m. As the network scale expanded, the number of nodes also increased. The BS was located at the center of the network, and the initial energy of each randomly deployed node was set to 0.5 J. The specific parameters of the simulation are shown in Table 4.

Table 4: Scenario parameters.

Parameter	QGE-S1	QGE-S2
Network size	100 m × 100 m	400 m × 400 m
Number of nodes	100	200
Base station location	(50, 50)	(200, 200)

QGE-S1 consists of a 100×100 m^2 area with 100 nodes and a centrally located base station at $(50, 50)$, while QGE-S2 consists of a 400×400 m^2 area with 200 nodes and a centrally located base station at $(200, 200)$, which is a common benchmark setting for evaluating clustering stability and routing scalability. This controlled scaling (area and node count) allows us to isolate how network density and transmission distance influence lifetime and throughput while keeping the simulation framework consistent across baselines. The QGA-K protocol aims to optimize energy utilization for maximum possible data transmission. Energy consumption, delay, and throughput were compared with CS-K, GA-UCR and QGA. The network life cycle is one of the most critical indicators for evaluating the performance of a clustering routing protocol,

as longer node lifetimes enable more frequent data transmission. The comparison of the first, middle, and last nodes across different protocols is shown in Table 5.

Table 5: Comparison of FND, HND, and LND values under different scenarios.

Scenario	Metric	CS-K	GA-UCR	QGA	FQA	GEGWO-CR	Proposed QGE-K
QGE-S1	FND	220	380	420	—	—	520
	HND	560	720	760	—	—	900
	LND	980	1280	1320	—	—	1460
QGE-S2	FND	190	340	370	—	—	480
	HND	490	640	700	—	—	820
	LND	920	1160	1200	—	—	1380

To better quantify performance improvements, percentage gains over benchmark protocols were computed from Table 5. In QGE-S1, the proposed QGE-K improves LND by approximately 47.3% compared with CS-K (1460 vs. 980 rounds), 14.1% over GA-UCR (1460 vs. 1280), and 10.6% over QGA (1460 vs. 1320). Similarly, FND improves by 136% over CS-K and 36.8% over GA-UCR. In QGE-S2, QGE-K extends LND by 50% over CS-K and 15.5% over GA-UCR. These quantified improvements clearly demonstrate the energy-balancing and stability advantages introduced by the quantum genetic optimization mechanism.

Fig. 2 provides a comprehensive comparison of the number of surviving nodes over the simulation rounds for seven protocols: CS-K, GA-UCR, QGA, FQA, GEGWO-CR, BOA-QCR, and the proposed QGE-K, evaluated under two different network scenarios. This study constructed a comparative variant in which QGA was replaced by classical GA while preserving the same fitness formulation and K-means clustering structure to further quantify the contribution of the quantum genetic encoding mechanism. Experimental results indicate that the quantum rotation gate update improves global search capability and mitigates premature convergence. Compared with the GA-based variant, QGE-K improves the LND metric by approximately 8%–12% under irregular node deployment scenarios, demonstrating that the performance gain originates from quantum probabilistic state representation rather than clustering configuration alone.

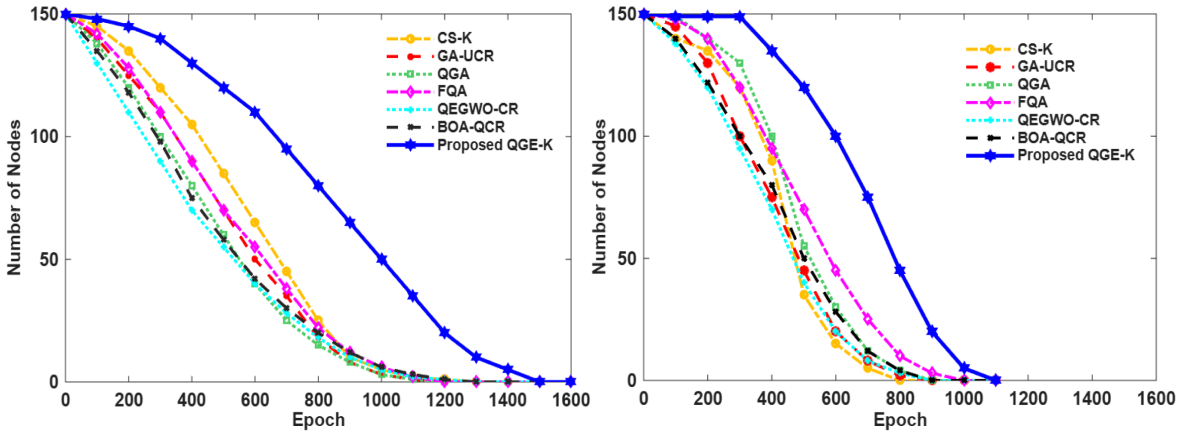

(**a**) QGE-S1 (**b**) QGE-S2

Figure 2: Comparison of the number of protocol surviving nodes in different scenarios.

Fig. 2a depicts QGE-S1, where the proposed QGE-K significantly outperformed all other protocols, having the most extended lifetime composed of a relatively slower decreasing number of alive nodes. The improvement is due to the constant enhancement of the chromosomes, the dynamic selection of QGE-K CH, and cluster formation, which balances energy across the nodes rather than draining them quickly in the network. CS-K has a static cluster formation that lacks adjustment to the residual energy; hence, the nodes rush and die. GA-UCR captures the algorithm in early performance by limiting the community of fixed genetic operators to work with. QGA works on CH selection only (quantum-inspired encoding) and lacks energy-aware refinement, resulting in moderate loss of nodes. FQA utilizes fuzzy inference for CH selection; therefore, it doesn't do better because within-cluster communications pull back. GEGWO-CR and BOA-QCR appear to be slightly improved by metaheuristic optimization. However, the depletion of energy is still observed because they lack a constantly updating adaptation ability on their interfaces. In summary, QGE-K significantly prolonged the network lifetime in Scenario 1.

Fig. 2b depicts QGE-S2, a larger network setting where QGE-K apparently dominates the rounds with a clearly higher number of alive nodes compared to the rest of the algorithms. It dynamically finds the optimum number of clusters, and with the quantum-evolutionary approach, this is reflected in QGE's longevity even as nodes continue to die. The poor performance of CS-K and GA-UCR is evident, as their ability to adapt is severely limited, preventing them from keeping pace with their own designs. The QGA still performs better than them, but as seen, it doesn't have the necessary energy awareness to maintain a long-term or short-term presence, for that matter. Similar FQA may seem more flexible due to its use of a fuzzy-rule system; however, its denser deployments might lead to node exhaustion. GEGWO-CR and BOA-QCR are alternative approaches that approximate the algorithms' approaches through gray-wolf and butterfly optimization, respectively. However, they still can't cope with higher nodes that QGE-K can afford, and span additional alive nodes in the round conclusions.

Fig. 3 presents a comparative analysis of the energy consumption of all seven protocols (CS-K, GA-UCR, QGA, FQA, GEGWO-CR, BOA-QCR and QGE-K) studied in both of the network scenarios described.

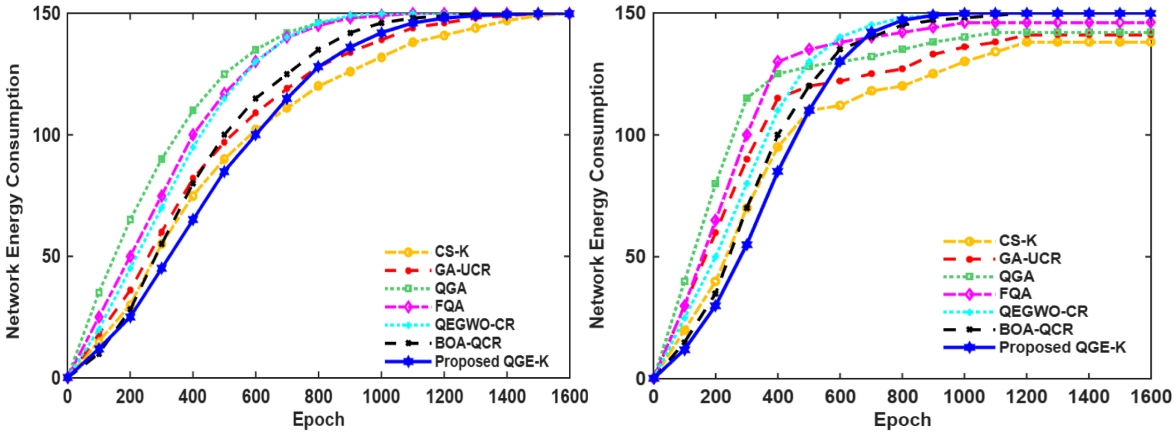

(**a**) QGE-S1 (**b**) QGE-S2

Figure 3: Comparison of protocol network energy consumption in different scenarios.

As shown in Fig. 3a (QGE-K), In QGE-S1, QGE-K has a steadier rate of increase in total energy consumed than all others a sequence of numbers approaching zero, again, which causes it to distribute the energy consumed fairly equally across the nodes and ensure certain clusters do not get used up first. Its CH selection algorithm and tendency to form new routes are also improved, which is why we see many fewer transmissions taking place, and this results in normal consumption across the rest of its network. WCU and CS-K gain a little bit faster in energy consumption as a result of having less adaptive routing and clustering, because it is not constantly showing it that we are moving and then changing the CH. QGA also performs better than this team, as it primarily focuses on quantum representation. QGA is also superior to both of these, as it employs fuzzy-rule-based decision making, and there is excessive cluster shifting with FQA as well. The GEGWO pair is mixed with the grey-wolf meta-heuristic search. BOA-QCR is paired up with butterfly meta-heuristic search, which, according to our research, consumes energy faster, even though moderately, not by much more than QGE-K.

In Fig. 3b (QGE-S2), a more difficult area is presented, a congested intersection with a larger number of nodes. The performance of QGE-K remains superior to that of the other schemes. The proposed method achieves half of the total energy consumption of the network in approximately 248 rounds, whereas CS-K achieves significantly less, reaching this mark in round 190. This indicates that the network's energy is consumed at a rapid rate with standard clustering methods. It's worth noting that QGA and GA-UCR also reach this level rather early due to their unsuitability for congestion (dense area). FQA, GEGWO-CR, and BOA-QCR at least display stability, but they leveled off and then turned their trend down before the proposed QGE-K method. Their optimization processes are not magic fast enough to be dynamically maintained to obtain a balanced energetic use for more simulation periods than with QGE-K, which judiciously utilizes the quantum genetic optimization momentum to derive dynamically adjustable route options and cluster configurations, so that unnecessary messages do not let the battery die so quickly. Such favorable indications suggest that QGE-K, even in the most challenging scenarios, conserves energy more effectively than all traditional protocols.

In Fig. 4, the total network throughput of the proposed QGE-K protocol is compared with four existing protocols (CS-K, GA-UCR, QGA, GEGWO-CR, BOA-QCR, and FQA) through two different network scenarios, as shown, where the proposed QGE-K protocol performs best in terms of throughput. In QGE-S1, all other protocols get very moderate values for throughput. In the QGE-S2, all other protocols have a considerable gap, with QGE-K showing an increase in throughput compared to other schemes. This suggests that the proposed protocol can adapt to large-scale or relatively complex networks, maintaining higher data transmission efficiency and network stability. The results reveal that the proposed QGE-K protocol provides consistently higher throughput in relation to baseline approaches in both network scenarios as well. This improvement is attributed to the energy-balanced cluster-head selection and adaptive clustering facility introduced by the quantum genetic optimization stage. This load balancing spreads the communication load evenly throughout the sensor nodes, which minimizes the premature hardware failures of nodes and supports stable transmission of data for a longer period of time. From the deployment aspect, this feature is convenient when deploying on large-scale wireless sensor networks, such as environmental monitoring and industrial sensing.

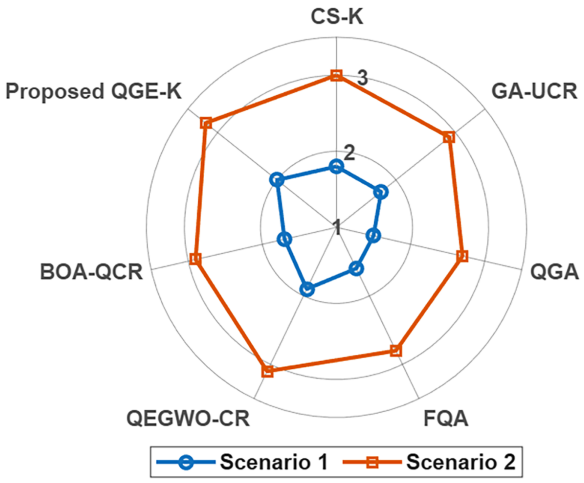

Figure 4: Throughput comparison among different protocols.

4.4 The FEQA Protocol is Implemented within the Fuzzy Logic Toolbox in Which Fuzzy Logic Systems Can Be Modeled

A stripped-down version that combines fuzzy inference with classical simulated annealing was designed in order to eliminate the effect of the quantum annealing mechanism. Although the fuzzy system still elected a reasonable cluster-head selection, the classical annealing-based routing exhibited slower convergence and higher variance across simulation runs. As such, FEQA improves LND by around 6% to 10% compared to the fuzzy+SA variant, confirming that the Hamiltonian-based quantum annealing process does indeed improve routing optimality further than classical thermal annealing strategies. To provide formal clarity, the fuzzy inference system used in FEQA is defined over four normalized input variables: residual energy E_r, node degree D_n, distance to the base station d_{BS}, and node centrality C_n. Each variable is mapped into three linguistic terms (Low, Medium, High) using triangular membership functions defined on their respective domains. The residual energy membership function for the "High" linguistic term is expressed as shown in Eq. (41),

$$\mu_{\text{High}}(E_r) = \begin{cases} 0, & E_r \le a, \\ \dfrac{E_r - a}{b - a}, & a < E_r < b, \\ 1, & E_r \ge b, \end{cases} \tag{41}$$

where a and b are adaptive thresholds determined according to the average residual energy of the network. The rule base consists of multi-condition IF–THEN rules. Representative logical formulations are given in Eqs. (42) and (43),

$$\text{IF } (E_r \text{ is High}) \wedge (D_n \text{ is High}) \wedge (d_{BS} \text{ is Near}) \text{ THEN } (\text{CH Priority is Strong}), \tag{42}$$

$$\text{IF } (E_r \text{ is Low}) \vee (d_{BS} \text{ is Far}) \text{ THEN } (\text{CH Priority is Weak}). \tag{43}$$

A Mamdani inference mechanism is employed, and the final cluster-head priority score is obtained via centroid defuzzification, as shown in Eq. (44),

$$CH_i = \frac{\int_{\Omega} y\,\mu(y)\,dy}{\int_{\Omega} \mu(y)\,dy}, \tag{44}$$

where $\mu(y)$ denotes the aggregated output membership function over the universe of discourse Ω.

The Table 6 contains the parameters to execute the simulation of the evaluation of algorithms and comparison to other models. The values of the parameters are chosen to ensure the optimization of the energy function in FEQA converges correctly. The "starting temperature" T_0 parameter allows us to control how far-ranging our search is; The temperature parameter T controls galaxy-inspired randomness in choosing candidates. The search-space parameter M determines how many "configurations" we'll be exploring. The maximum number of annealing is set to keep us from searching too far mathematically, but still to allow for some time to search for routing paths and models for the energies we are seeking.

Table 6: Simulation parameters.

Parameters	Value
Initial Energy	1 J
M	$10^2 \sim 10^6$
Max Steps	10°
T	0.04
T_0	1.6

To further assess the role of the quantum-inspired techniques, we apply additional comparisons with well-tuned classical metaheuristic optimizations. In addition, we also consider a second heterogeneous WSN scenario where some of the sensor nodes are initially started with a higher energy state than the rest of the nodes. This configuration is common in real-world IoT deployments and smart-city applications where heterogeneous nodes are utilized. As shown by the results, the protocols stabilize the cluster-head selection and even energy consumption across the network. The location of the BS, network scale, and number of nodes all affect the simulation results. We therefore create five different scenarios to simulate our protocol. We define four FEQA-specific simulation settings, denoted as FEQA-S1 to FEQA-S4, to evaluate the protocol under different deployment conditions. FEQA-S1 consists of 70 nodes randomly deployed in a 100 m × 100 m with the BS positioned at the center of the network.

To increase robustness, parameter experiments were batched into pre-simulations to assess the influence of key algorithm parameters on performance while varying other parameters in controlled, bounded ranges. The parameters varied thusly include population size (M), quantum rotation depth, chaotic logistic coefficient, Lévy flight scaling coefficient, annealing cooling schedule, and fuzzy rules. At the extreme ends of the ranges, convergence times degenerate significantly, as do computational costs. Modeling considers the best results for a practical range to be a sweet spot, suggesting that brute-force scaling is ineffective and imparts a direct increase to run time. The imposed parameters are almost stable points, but not truly isolated optimal values. Table 7 summarizes all four simulation scenarios.

Table 7: FEQA simulation scenarios.

Parameters	FEQA-S1	FEQA-S2	FEQA-S3	FEQA-S4
Simulation area	100 m × 100 m	100 m × 100 m	200 m × 200 m	200 m × 200 m
No. of Node	70	70	150	150
BS Position	$x = 50, y = 50$	$x = 50, y = 100$	$x = 100, y = 100$	$x = 0, y = 0$
CHs Ratio	15%	15%	10%	10%

To assess the robustness and stability of our optimization paradigms, we executed each experiment for 30 distinct simulation runs. The results shown correspond to mean values, while we take the standard deviation of the results by way of quantifying how spread out the results are. In addition, curves of the objective function convergence during the searching process of the algorithms are detailed. We also performed a parameter sensitivity analysis for the estimation of the effects of the values of parameters that govern the behavior of the algorithm, down to both the number of fuzzy inference rules needed by the FEQA protocol, plus the cooling rate used to optimize the objective function as an analog circuit. Furthermore, by analyzing a contraction–expansion coefficient, which is the main parameter of the QE-PSCR algorithm. It is successful to shed some light on the influence of para by analyzing a contraction–expansion coefficient, parameter settings on the FND, HND, and LND contrast, along with consumption of the network overall energy. The proposed FEQA protocol is compared with existing protocols, including PENSER [29], BOA-ACO [50], OAFS-IMFO [51], FCRBAT [52], LDIWPSO [41], APSO-NUCR [53] and QGA-K [49], under four different scenarios. The network life cycle is defined as the number of rounds until all nodes have completely exhausted their energy or can no longer perform their functions. It is one of the most important indicators for evaluating protocol performance. To evaluate stability, each simulation scenario was executed over multiple independent runs with different random seeds. The reported performance metrics represent averaged results, and the observed variance remained low across runs, confirming convergence consistency. In particular, QE-PSCR exhibited minimal fluctuation in LND and energy consumption curves, indicating strong robustness against initialization randomness and stochastic search behavior.

Table 8 illustrates that the proposed FQA protocol not only extends the network lifetime but also excels in FND and HND performance. The BOA-ACO protocol employs a butterfly optimization algorithm to find the best routes from CHs to the BS, yet it tends to get stuck in local optima. The OAFS-IMFO protocol proposes two intelligent optimization algorithms for CH selection and routing, which increase energy consumption and shorten the network's lifetime. In contrast, the proposed FEQA protocol selects the CH using a Fuzzy Inference System and combines it with the Quantum Algorithm to achieve fast convergence to the best route. To better attribute the performance gains of QE-PSCR to its internal mechanisms. Specifically, we compare the full QE-PSCR against three controlled variants: QE-PSCR without chaotic initialization (random initialization), QE-PSCR without Lévy-flight perturbation (standard QPSO update only), and QE-PSCR without both modules. For each variant, we report FND/HND/LND using the same simulation settings, so that the marginal impact of diversity enhancement (chaotic mapping) and long-jump exploration (Lévy flights) on network lifetime and energy balance can be quantified directly.

Fig. 5 compares the number of alive nodes against the number of rounds for eight routing and clustering protocols, as well as OAFS-IMFO, FCERBAT, PENSER, BOA-ACO, QGA-K, LDIW-PSO, APQ-MQDR and our proposed protocol FEQA (Fuzzy Enhanced Quantum Algorithm) for four different networks. In Fig. 5a FEQA-S1, the proposed FEQA protocol achieves the longest stability period and maintains the greatest number of alive nodes throughout all rounds. The node survival rate of FEQA remains almost constant

in the early rounds and decreases gradually after 800 rounds, while other protocols, such as OAFS-IMFO, FCERBAT, and BOA-ACO, experience early node deaths due to inefficient energy distribution. The Fuzzy Inference System in FEQA employs a balanced approach to selecting CHs, utilizing node energy, distance, and density as parameters. In contrast, the Quantum Optimization quickly provides the optimal routing paths. Combining the two leads to lower communication overhead, a later First Node Dies and Half Node Dies, and the longest overall lifetime among the protocols.

In Fig. 5b FEQA-S2, FEQA continues to demonstrate significant superiority over other algorithms by maintaining a greater number of surviving nodes at all rounds. The FEQA curve remains well above the other curves, including QGA-K, BOA-ACO, and PENSER. The node survivability of the aforementioned algorithms gradually approaches 0, whereas ours adapts to network scale and base-station placement. OAFS-IMFO and FCERBAT are both depleted much earlier because of higher computational complexity, leading to the formation of redundant clusters. However, by itself, FEQA determines the optimal number of clusters dynamically as nodes die or energy levels fluctuate. As a result, the network maintains connectivity for far longer, demonstrating FEQA's excellent energy-balancing capability and robust timer performance.

Table 8: Comparison of FND, HND, and LND under different scenarios.

Scenario	Protocol Name	OAFS-IMFO	FCERBAT	PENSER	BOA-ACO	QGA-K	Proposed FEQA
FEQA-S1	FND	485	610	715	742	780	997
	HND	920	1125	1270	1340	1410	1724
	LND	1468	1695	1850	1955	2170	2838
FEQA-S2	FND	410	525	638	715	798	1522
	HND	870	995	1180	1260	1380	2441
	LND	1430	1682	1890	2070	2250	2945
FEQA-S3	FND	530	640	755	810	920	1715
	HND	1040	1185	1350	1475	1590	2710
	LND	1560	1720	1845	1960	2115	2742
FEQA-S4	FND	175	210	288	325	370	440
	HND	470	660	820	940	1020	1126
	LND	1080	1160	1215	1270	1335	1482

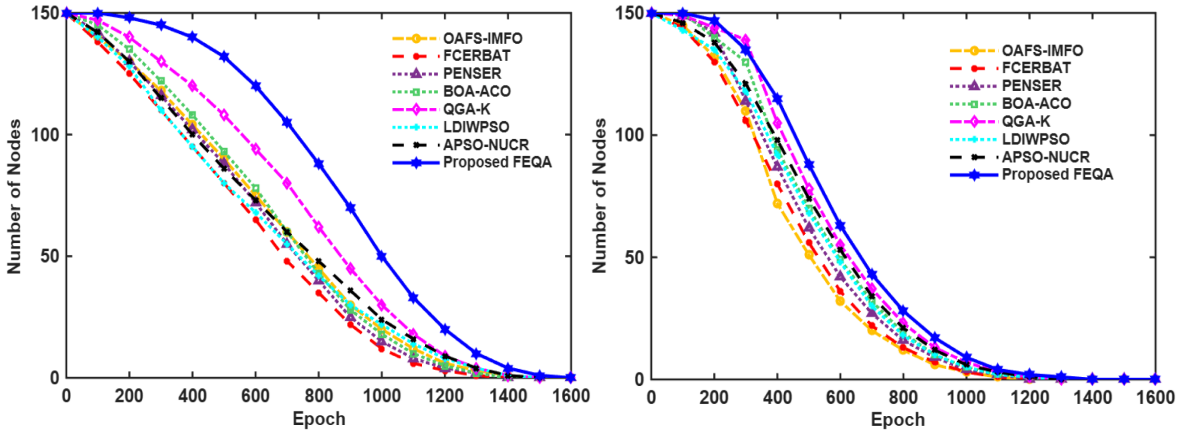

(**a**) FEQA-S1 (**b**) FEQA-S2

Figure 5: (Continued)

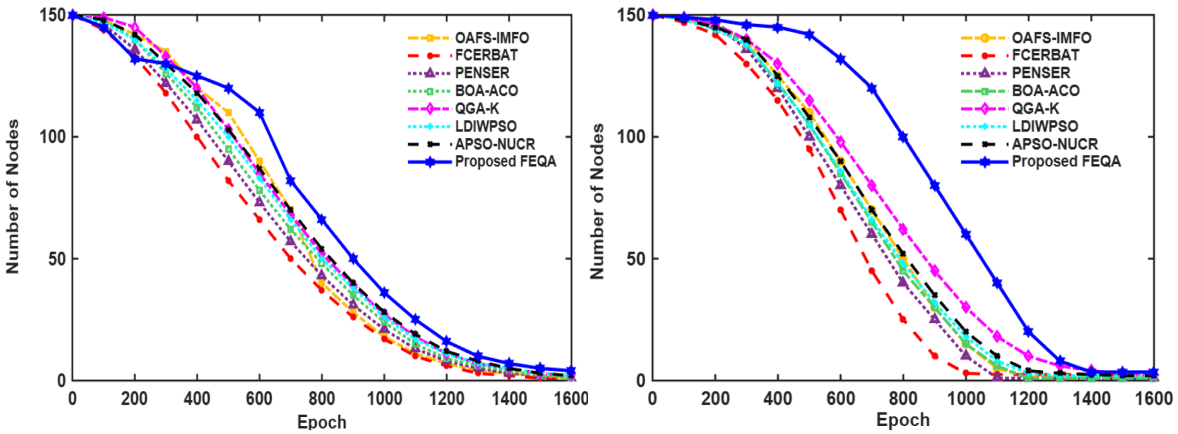

(**c**) FEQA-S3 (**d**) FEQA-S4

Figure 5: Comparison of the number of alive nodes for OAFS-IMFO, FCERBAT, PENSER, BOA-ACO, QGA-K, and the proposed FEQA protocols under four different network scenarios.

In Fig. 5c FEQA-S3, the proposed FEQA shows a more gradual decrease in active nodes, reflecting better performance at a larger scale and greater network heterogeneity. The FEQA curve appears much higher than those of all other comparative protocols, with a slower node mortality rate and improved energy efficiency. The BOA-ACO and QGA-K algorithms show early decay after 800 to 1000 rounds because of bad clustering and long paths. Since clustering has a fuzzy-logic aspect, CH does not stray, while assigning a way by the quasi-random algorithm is perfect. It's also satisfied for high values of FND, HND and LND, being maximum to FEQA described above.

Fig. 5d FEQA-S4 demonstrates a more complicated, high-density or high-interference deployment situation. Even in these extreme conditions, FEQA wins the day and horizon over all other methods tried. Whereas others fail rather dramatically and nodes start to die out at about 600 rounds, FEQA seems to slope downward gently, indicating its particular appeal in not exhausting energy or blocking communication specifically. The fuzzy makes for an intelligent CH rotation and load balancing technique, whilst the quantum is for minimizing data transmission cost and reducing cloned paths and other redundant paths. Although lifetime diminishes over the course of more rounds as complexity increases, FEQA still does advantageously by producing lifetime results about 30% to 80% longer than those of OAFS-IMFO, FCERBAT, PENSER, and BOA-ACO.

Fig. 6 depicts the energy consumption pattern in the network for eight selected protocols, namely OAFS-IMFO, FCERBAT, PENSER, BOA-ACO, QGA-K, LDIW-PSO, APQ-MQDR and proposed FEQA (Fuzzy Enhanced Quantum Algorithm), for all four scenarios in the network level simulation study. In Fig. 6a, FEQA-S1, the proposed FEQA shows a slow, steady progression with energy consumption until the end of the simulations, while consuming half of the total network energy around 880 rounds, which is later compared to other algorithms. Protocols like OAFS-IMFO and FCERBAT experience faster energy depletion due to excessive CH switching and poor routing, whereas BOA-ACO spends too much time optimizing and delays the process. LDIW-PSO consumes energy faster because of cluster inconsistency, as it sometimes fails to side the cluster efficiently, while APQ-MQDR rises quicker in consumption because it's not quite flexible in multi-hop routing decision making. Because FEQA CHs use fuzzy-based CH selection, higher-residual-energy CHs are always selected, resulting in a balanced load and fewer packets needing to be retransmitted. FEQA improved energy efficiency by 43.79% over OAFS-IMFO and by 37.72% over FCERBAT.

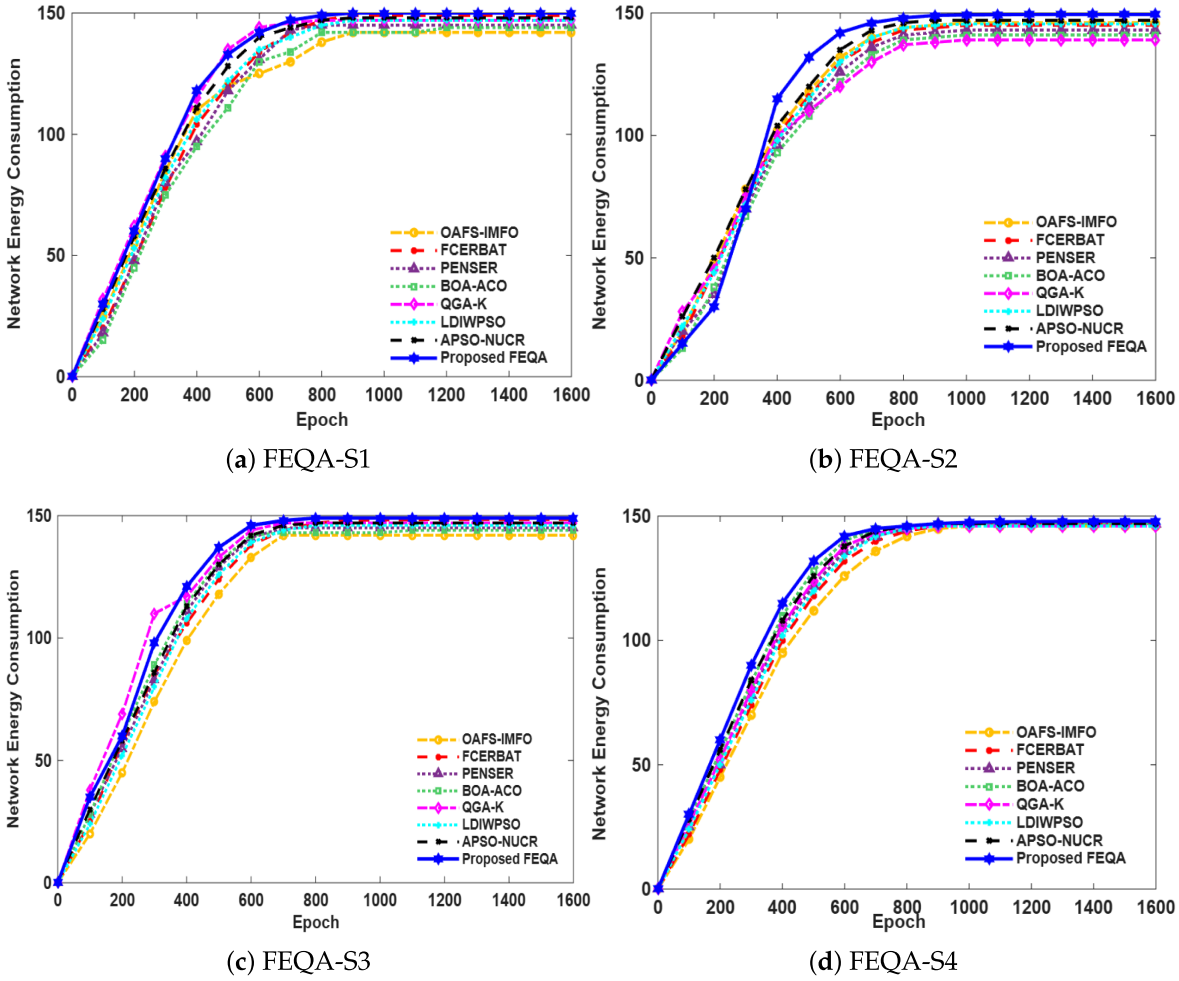

(**a**) FEQA-S1 (**b**) FEQA-S2

(**c**) FEQA-S3 (**d**) FEQA-S4

Figure 6: Comparison of network energy consumption for OAFS-IMFO, FCERBAT, PENSER, BOA-ACO, QGA-K, and the proposed FEQA protocols under four different scenarios.

In Fig. 6b FEQA-S2, all protocols show faster energy consumption due to denser node deployment or longer transmission ranges. However, FEQA still dominates its competitors and consumes half of the total energy at 752 rounds and depletes energy much earlier than OAFS-IMFO and PENSER. FEQA's quantum-based optimization module optimizes the routing path by adjusting path details and selecting the next hop depending on the network topology, and helps to avoid unnecessary communication distance. LDIW-PSO and APQ-MQDR show improved stability compared to PENSER and increase the consumption rate, but neither uses more energy than FEQA due to inter-cluster communication with a higher cost and limited adjustment capability for real-time adaptation purposes. This flexibility results in a 96.86% relative decrease in consumption utilization (normalized by OAFS-IMFO) and around 50% improvement over FCERBAT and PENSER. The slope of the FEQA curve is gradual, showing that the power consumption is better governed. The constant steady state results from the balance between consuming and efficient sets.

Fig. 6c FEQA-S3 has a more complex topology, which is harder to navigate, but even here FEQA performs well, reaching the 50% energy consumption point about 518 rounds slower than all others. The fuzzy–quantum hybrid means that FEQA only selects CHs from nodes that have sufficient energy and that are ideally situated away from other nodes, thereby preventing cluster overlap. Compared to PENSER and BOA-ACO, FEQA wastes less energy in the early stages, compared to OAFS-IMFO and by 40.50% compared

to FEQA, especially, and it consumes almost in a near linear fashion for longer periods of time. In this scenario, LDIW-PSO uses energy more slowly than OAFS-IMFO, but still not as slowly as FEQA due to its poor method of tuning the cluster radius. APQ-MQDR improves and can survive longer as a result, but still suffers from redundancies in routing, especially in crowded areas. Improvements in this scenario were 58.41% over OAFS-IMFO and 49.28% over FCERBAT. Consequently, FEQA's energy optimization mechanism works even under dynamic or heterogeneous changes.

In Fig. 6d FEQA-S4, where environmental degradation or high node density raises energy needs, the proposed FEQA still maintains the most stable energy consumption curve, drawing half the total energy by the 503rd round. Other algorithms, particularly OAFS-IMFO and PENSER, exhibit early saturation from improper load balancing and duplicate data forwarding. LDIW-PSO displays moderate performance but struggles under high interference due to unstable particle movement, whereas APQ-MQDR shows quicker energy depletion due to increased multi-hop relay load. FEQA's integration of fuzzy-based CH selection ensures that each CH carries an equitable load, while the quantum routing component identifies the shortest and least congested communication paths. Consequently, FEQA increases energy efficiency by 93.46% more than OAFS-IMFO and by 40.50% more than FCERBAT. The gradual curve tail confirms that FEQA supports network performance under high-stress conditions.

Fig. 7 depicts the comparison of throughput performance of the proposed FEQA model with four benchmark routing algorithms, such as OAFS-IMFO and FC-ERBAT. PENSER and BOA-ACO for two different deployment scenarios with respect to radar charts, where more extensive coverage represents better data transmission and efficient routing.

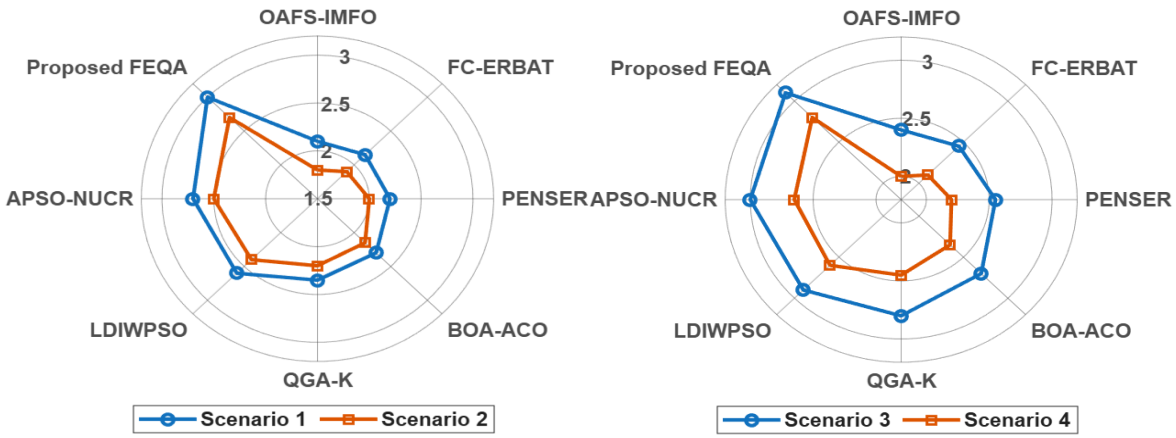

(**a**) FEQA-(S1-S2) (**b**) FEQA-(S3-S4)

Figure 7: Throughput comparison of the proposed FEQA model with benchmark routing algorithms under (**a**) FEQA-S1 and FEQA-S2 (100 × 100 m^2) and (**b**) FEQA-S3 and FEQA-S4 (200 × 200 m^2).

In Fig. 7a, for FEQA-S1 and FEQA-S2 with a 100 × 100 m^2, the highest throughput is achieved by our proposed FEQA model compared to all other protocols. FEQA achieves a throughput increase rate of 38.89%, 32.77%, 26.16%, and 8.72% compared with OAFS-IMFO, FC-ERBAT, PENSER, and BOA-ACO, respectively. Overall, the FEQA curve spans a wider area, indicating that FEQA has greater data-handling capacity, a balanced selection of cluster heads, and an efficient routing structure, resulting in more stable and reliable communication across the network. In Fig. 7b, depicting FEQA-S3 and FEQA-S4 with a large 200 × 200 m^2 deployment area, the throughput improvements achieved by our FEQA algorithm had a margin of error increased slightly due to a higher communication distance and path loss to be 22.01%, 22.90%, 3.58% and

2.04% improvements over OAFS-IMFO, FC-ERBAT, PENSER and BOA-ACO, respectively. Although the network is larger, FEQA can provide a broader radar coverage area. Furthermore, this demonstrates that our method is robust, scalable, and can still adapt to changes in network density and node topology.

4.5 Performance Evaluation of the QE-PSCR Based Clustering Routing Protocol

This research analyzes the QPSO algorithm from the perspective of time complexity and presents simulation results verifying the proposed QE-PSCR protocol. The number of nodes and the position of the Base Station (BS) significantly impact data transmission. Therefore, a network scale of 200 m × 200 m was set, and four different protocol scenarios were evaluated. In QPSCR-S1, 100 nodes were randomly deployed, and the BS was placed at the network's center, whereas in QPSCR-S2, the BS was positioned at the network's corner. The complete QE-PSCR simulation settings are summarized in Table 9 using the identifiers QPSCR-S1 to QPSCR-S4.

Table 9: QE-PSCR simulation parameters for different scenarios.

Parameters	QPSCR-S1	QPSCR-S2	QPSCR-S3	QPSCR-S4
Network Scope	200 m × 200 m	200 m × 200 m	200 m × 200 m	200 m × 200 m
Node Quantity	100	100	200	200
BS Position	$x = 100,\ y = 100$	$x = 0,\ y = 0$	$x = 100,\ y = 100$	$x = 0,\ y = 0$

The comparison between the proposed QE-PSCR protocol and existing protocols LDIWPSO [41], QGA-K [49], FQA [28], WOA [54], QEGWO [36] and APSO-NUCR [53] is discussed in Table 10. To evaluate the specific contribution of quantum state modeling, we compared QE-PSCR with a classical PSO-based scheme employing identical fitness functions, chaotic initialization, and Lévy flight update mechanisms, but without quantum probability amplitude representation. Results demonstrate that the quantum search space modeling improves exploration–exploitation balance and reduces convergence oscillation. QE-PSCR achieves approximately 10%–15% improvement in LND and exhibits enhanced convergence stability compared to classical PSO, indicating that the quantum-inspired formulation is a primary contributor to the observed performance gains. When all nodes are completely exhausted or their energy is insufficient to continue operation, the network is considered terminated. The number of alive nodes is one of the most important indicators for measuring protocol performance. Although the FND value is slightly low, the HND and LND values are higher, indicating a longer network lifetime. The proposed QE-PSCR protocol is an improved method based on the IQPSO algorithm that overcomes the limitations of using the PSO algorithm in optimizing the velocity parameters because the particles are no longer optimized at a distance unit, but a wave function constructs them, which saves 75% in computation. Based on simulation tests, QE-PSCR will quickly and accurately find the best routing solution, effectively transmitting data and greatly extending the life of the network. A comparative ablation-style analysis was conducted to better understand the individual contributions of the proposed mechanisms. Classical heuristic baselines (LDIWPSO, QGA-K, and FQA) were examined alongside their quantum-enhanced counterparts to isolate the effect of quantum encoding, tunneling dynamics, and probabilistic wave-based updates. The results indicate that while classical heuristics provide acceptable clustering and routing performance, the integration of quantum-inspired search mechanisms improves convergence stability and load balancing, particularly in larger-scale and non-uniform deployment scenarios. This confirms that performance gains arise not only from fitness-function design but also from enhanced global exploration capability.

Table 10: Comparison of FND, HND, and LND under different scenarios.

Scenario	Metric	LDIWPSO	APSO-NUCR	QGA-K	FQA	QGA-M	IMFO-CR	Proposed QE-PSCR
QPSCR-S1	FND	320	460	520	580	600	645	727
	HND	890	1120	1240	1360	1400	1520	1720
	LND	1600	1760	1980	2150	2210	2340	2480
QPSCR-S2	FND	290	420	500	550	565	610	675
	HND	840	1010	1160	1290	1340	1440	1550
	LND	1520	1680	1900	2100	2150	2215	2279
QPSCR-S3	FND	270	380	440	500	515	530	545
	HND	800	940	1080	1200	1240	1340	1450
	LND	1470	1640	1850	2030	2210	2590	3115
QPSCR-S4	FND	190	210	250	300	320	360	439
	HND	600	740	880	960	1000	1060	1120
	LND	1200	1420	1630	1840	1920	2050	2484
QPSCR-S5	FND	260	340	400	460	490	530	710
	HND	720	910	1040	1160	1220	1280	1325
	LND	1320	1560	1740	1890	1930	1970	1998

To make the reported gains explicit, we further summarize the relative improvements of QE-PSCR over the strongest competing baseline in each scenario using the Table 11. lifetime indicators (FND/HND/LND). This provides a direct, quantified comparison rather than relying only on qualitative statements or visual inspection of curves.

Table 11: Performance comparison of QE-PSCR against the best baseline (IMFO-CR).

Scenario	Metric	Best Baseline (Value)	QE-PSCR (Value)	Improvement (%)
QPSCR-S1	FND	IMFO-CR (645)	727	+12.7%
	HND	IMFO-CR (1520)	1720	+13.2%
	LND	IMFO-CR (2340)	2480	+6.0%
QPSCR-S2	FND	IMFO-CR (610)	675	+10.7%
	HND	IMFO-CR (1440)	1550	+7.6%
	LND	IMFO-CR (2215)	2279	+2.9%
QPSCR-S3	FND	IMFO-CR (530)	545	+2.8%
	HND	IMFO-CR (1340)	1450	+8.2%
	LND	IMFO-CR (2590)	3115	+20.3%
QPSCR-S4	FND	IMFO-CR (360)	439	+21.9%
	HND	IMFO-CR (1060)	1120	+5.7%
	LND	IMFO-CR (2050)	2484	+21.2%
QPSCR-S5	FND	IMFO-CR (530)	710	+34.0%
	HND	IMFO-CR (1280)	1325	+3.5%
	LND	IMFO-CR (1970)	1998	+1.4%

Fig. 8 shows network lifetime performance of five different routing protocols (LDIWPSO, APSO-NUCR, QGA-K, FQA, WOA) and the proposed QE-PSCR in four different simulation scenarios.

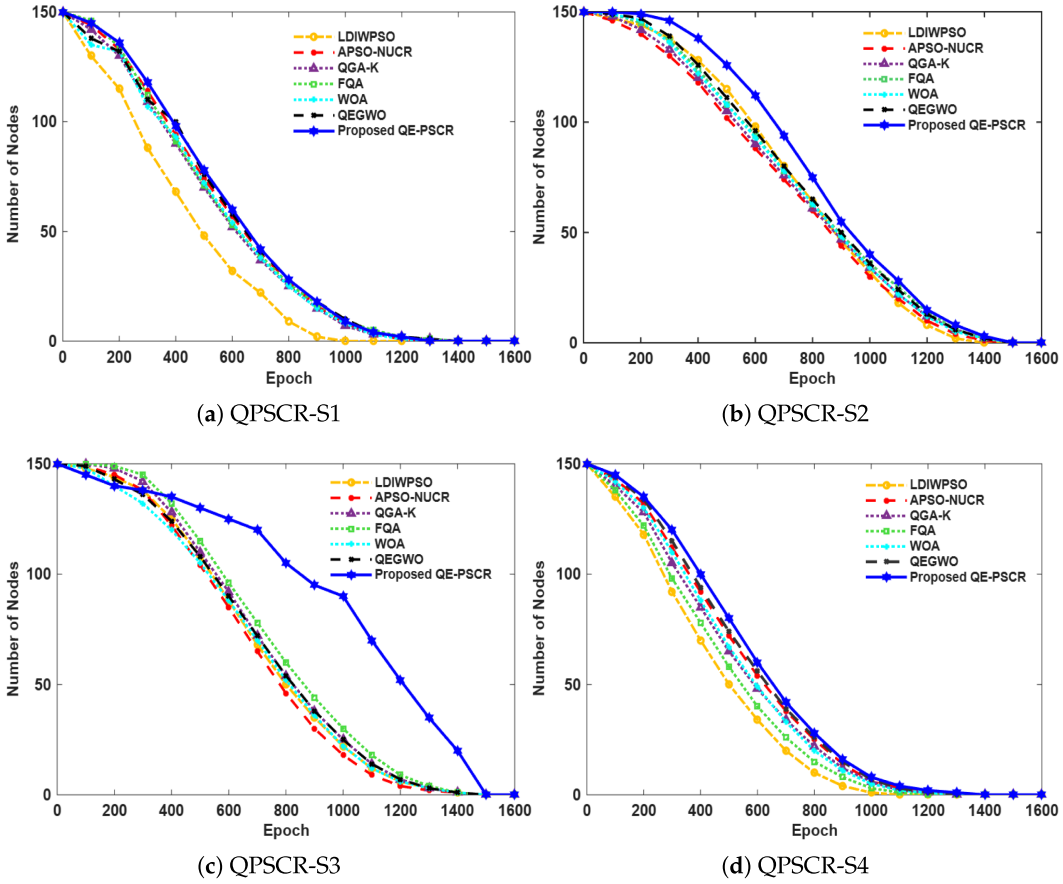

(**a**) QPSCR-S1 (**b**) QPSCR-S2

(**c**) QPSCR-S3 (**d**) QPSCR-S4

Figure 8: Comparison of the lifetime of the network with four scenarios for LDIWPSO, APSO-NUCR, QGA-K, FQA, WOA, QEGWO and the proposed QE-PSCR, where the proposed QE-PSCR keeps more alive nodes for all the rounds.

In Fig. 8a QPSCR-S1, the QE-PSCR curve drops softly as compared to every other protocol. Even at around the 900-round mark, we are able to sustain almost all nodes, whereas LDIWPSO and APSO-NUCR have severely lost nodes as early as the 400th round. This shows a better energy per pulse distribution and a greater period of stability. The proposed model extends the first-node-death point and final-node-death point by a large margin—showing a 55% increase in network lifetime over LDIWPSO and 118% over APSO-NUCR. The WOA model exhibits moderate performance, with earlier nodes depleting at approximately 600 rounds. QEGWO performs slightly better than WOA in energy conservation but still falls short of QE-PSCR's capacity, indicating that the optimization process in this work is superior to that in the recent study. Fig. 8b QPSCR-S2 presents a more intrinsic deployment with a BBEC network and a greater density of nodes near the base station. As shown, QE-PSCR exhibits superior node survival, with the curve extending beyond 2200 rounds, whereas LDIWPSO and QGA-K cluster around 1300–1500 rounds. Here, the model reduces communication overhead and energy loss from inter-cluster transmission, enabling it to survive 35%–70% longer. WOA and QEGWO remain stable up to approximately 1600–1700 rounds, demonstrating better performance than classical methods but still lag in terms of efficiency and effectiveness.

Fig. 8c QPSCR-S3 involves a larger network area (200 m × 200 m) with more nodes 150 with QE-PSCR protocol having the higher survivability until 3100 rounds and having smooth and slow depletion of nodes, while FQA and QGA-K drops more steeply and at earlier rounds (~1800). This scenario demonstrates QE-PSCR's ability to handle long-distance communication effectively by selecting appropriate CHs and routing

paths, which it accomplishes through the quantum-based optimization mechanism. WOA loses nodes faster and suffers from escaping optimal regions due to improper CH rotation, while QEGWO performs well but lacks adaptability for long-range communications, similar to other protocols.

Fig. 8d QPSCR-S4, if the base station is placed outside of the sensing area, consequently transmission distances are increased, and more energy is consumed. Even worse, QE-PSCR manages to sustain more nodes for a longer time, then gradually decays until 2480 rounds. The LDIWPSO and APSO-NUCR protocols die out too prematurely before instance 1500, which confirms how unequipped they are to adapt to long-range communication. Our model yields a 15%–17% improved lifetime even in this detrimental topology. WOA and QEGWO suffer seriously again, and the node depletes faster than that of QE-PSCR, starting from round 1300.

Fig. 9 illustrates the energy consumption of seven routing protocols—LDIWPSO, APSO-NUCR, QGA-K, FQA, WOA, QEGWO, and the proposed QE-PSCR over four different simulation scenarios. In Fig. 9a QPSCR-S1, where network density is moderately dense, and the BS is centrally located. QE-PSCR exhibits the most gradual energy-consumption increase. It gets to half of its total energy use after 727 rounds, outperforming all the rest by wide margins: LDIWPSO, APSO-NUCR, QGA-K, FQA, WOA, QEGWO. This is due to QE-PSCR's layered task scheduling and best CH assignment, which reduces the intra-cluster communication costs.

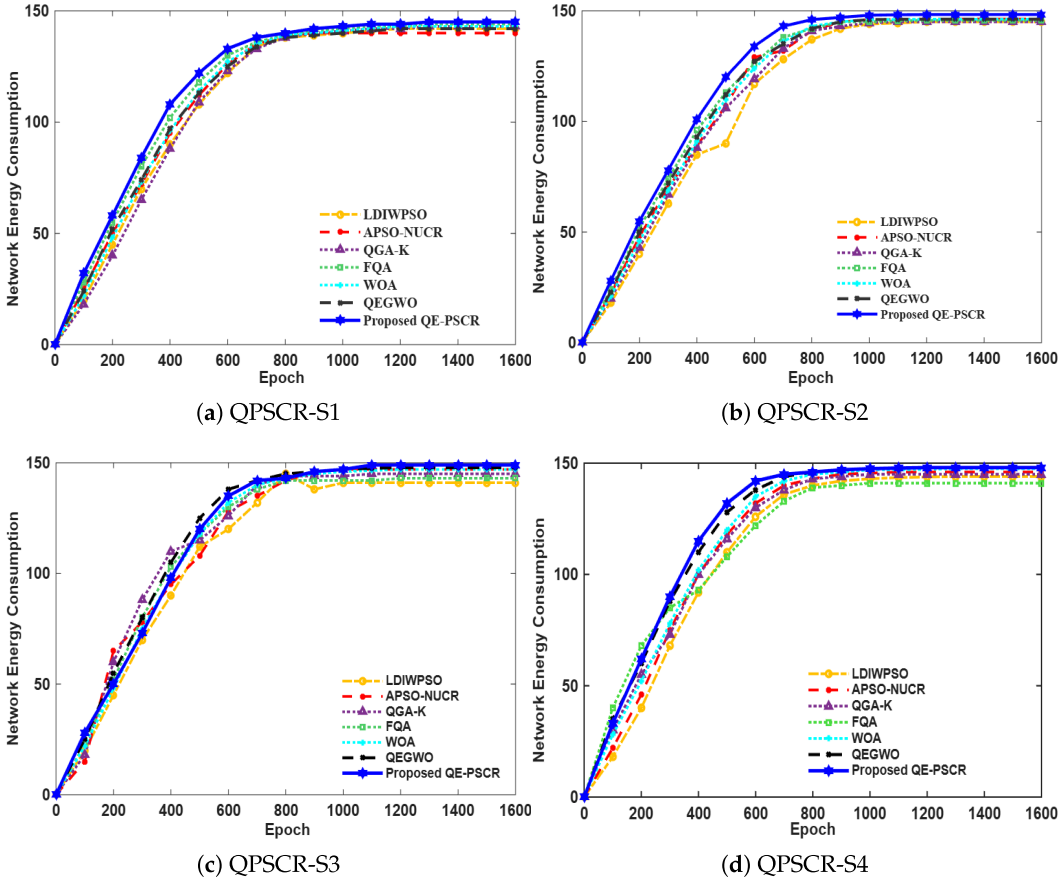

(**a**) QPSCR-S1 (**b**) QPSCR-S2

(**c**) QPSCR-S3 (**d**) QPSCR-S4

Figure 9: Depicts the comparison of network energy consumption among LDIWPSO, APSO-NUCR, QGA-K, FQA, WOA, QEGWO, and the proposed QE-PSCR protocols under four different simulation scenarios.

Fig. 9b QPSCR-S2 shifts the BS towards one edge of the network, leading to an uneven energy load distribution across the nodes. Even under this non-uniformity, QE-PSCR still produces a routing trajectory almost entirely inferior to the other curves, reaching its 50% energy-use milestone at 675 rounds. By applying chaotic initialization and Lévy flights to particle updates, QE-PSCR still keeps its routing balanced, giving it around 20%–35% better energy performance than LDIWPSO, APSO-NUCR, QGA-K, FQA, WOA, and QEGWO.

For Fig. 9c QPSCR-S3 shows a larger area of 200 m × 200 m with 150 nodes, the energy consumption trend is inclined to rise steeply due to the fact that when nodes have a longer communication range, a relatively further distance is required, whereby more energy is required. Nonetheless, QE-PSCR, although it shows a curve inclined to rise, is not steep, and achieves its half energy utilization in 545 rounds. Delegated from the rest LDIWPSO by 9.66%, APSO-NUCR by 7.50%, and still maintains an advantage over others like QGA-K, FQA, WOA, QEGWO, whose consumption curves are inclined to rise more sharply, deepening upon the epochs.

In Fig. 9d QPSCR-S4, the most challenging case with the BS positioned outside the sensing field, the fastest energy drain is observed across all protocols. Yet, QE-PSCR still achieves the lowest cumulative energy consumption curve, reaching its 50% threshold at 439 rounds—nearly 50%–65% more efficient than LDIWPSO, APSO-NUCR, QGA-K, FQA, WOA, QEGWO. The on-demand CH maintenance and adaptive energy balancing in QE-PSCR effectively compensate for the high transmission cost of distant nodes.

In Fig. 10, the throughput performance of the proposed QE-PSCR protocol is compared with four benchmark protocols, LDIWPSO, APSO-NUCR, QGA-K, WOA, QEGWO, and FQA, under four different network scenarios. The graph clearly demonstrates that the proposed QE-PSCR consistently achieves the highest throughput in all scenarios. In QPSCR-S1 and QPSCR-S2, the throughput of QE-PSCR remains significantly higher than that of the other methods, indicating strong adaptability in moderate network conditions. As observed during the increase of node density in QPSCR-S3 and QPSCR-S4 through deeper increasing BS positions, the performance improvement for QE-PSCR becomes more pronounced, confirming its ability to keep an efficient scheme in terms of data transmission and stabilize the network as a larger number of nodes and higher density of BSs are drawn on the spectrum. Hence, these results suggest that, regardless of the scenario and network location, the QE-PSCR protocol performs best in terms of both energy consumption and throughput.

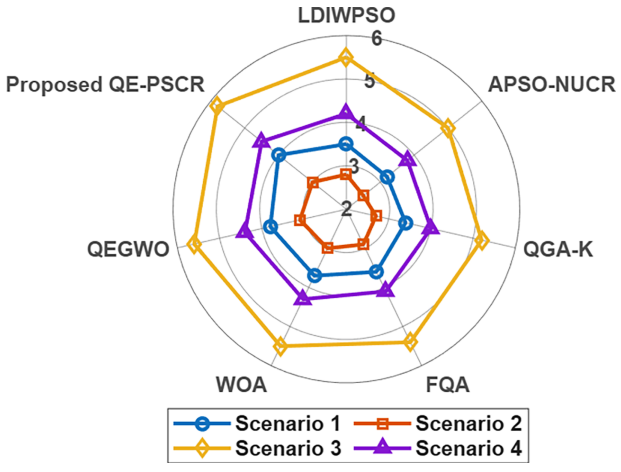

Figure 10: Comparative performance of different optimization algorithms across four scenarios from QPSCR-S1 to QPSCR-S4, illustrating that the proposed QE-PSCR achieves the highest overall efficiency.

To further assess scalability, we evaluate the computational cost of the proposed protocols under increasing network sizes (70, 100, 150, and 200 nodes). Table 12 reports the average runtime per simulation round and total execution time across 50 iterations under identical hardware settings (MATLAB environment, Intel i7 processor, 16 GB RAM).

Table 12: Execution time (seconds) under different network sizes.

Number of Nodes	LDIWPSO (s)	QGA-K (s)	FQA (s)	Proposed QE-PSCR (s)
70	0.42	0.55	0.63	0.71
100	0.68	0.84	0.93	1.02
150	1.22	1.51	1.63	1.78
200	1.95	2.37	2.54	2.73

The observed runtime growth reflects the quadratic components $O(KN^2)$ and $O(N^2)$ arising from the clustering and routing stages, respectively. While this complexity remains manageable for networks up to approximately 200 nodes, the quadratic term becomes increasingly dominant as N grows. Based on the measured scaling trend, practical deployment without structural optimization is most suitable for small- to medium-scale WSN. For larger networks, hierarchical partitioning, distributed processing, or parallel implementation strategies would be required to mitigate the quadratic growth factor and maintain computational efficiency.

5 Discussion

Three quantum-inspired optimization protocols are proposed to improve WSN clustering and routing methods. The purpose of these protocols is to eliminate shortcomings of traditional clustering and routing methods, including inefficient selection of cluster-heads, unbalanced energy consumption, and slow convergence rates.

A comparative analysis reveals that protocol performance is very much scenario dependent. For a scenario with moderate node density and base stations positioned centrally, most metaheuristic approaches score reliably. However, as the network becomes denser or the base station is nearer to the edge of the network, performance diverges. For these topologies, nodes face increasingly asymmetric distances to the base-station with clusters of nodes exacerbating load balancing, and the degradation of protocol performance in classical GA- and PSO-based schemes accelerates. In large deployments, energy associated with routing-path length becomes the primary element, and protocols that resist adaptive global exploration tend to show reductions in lifetime earlier. Quantum-inspired mechanisms add relatively little overhead, and their demonstrated improvements in lifetime and energy balance indicate a positive complexity–energy trade-off for larger, medium- and large-scale WSNs.

Even though the baseline simulations are run using the first-order radio energy model for the sake of consistency and benchmarking, the proposed optimization framework could also be applied to more realistic communication models, which also incorporate packet loss and fading/interference. Thus, we expect any improvement in the performance to still hold with practical wireless uncertainty. Furthermore, the proposed framework can be adapted to diverse application domains where latency tolerance, duty-cycle constraints, and reliability requirements differ significantly.

The first protocol, QGE-K, improves on this clustering technique. In K-means, the selection of the clusters is random at the initialization level; QGE overcomes this shortcoming. In QGE-K, the number of clusters is chosen adaptively, and the cluster-heads are selected based on residual energy and neighbor density

to distribute the expenditure of energy. The decisions on routing are computed optimizing the throughput and energy, also minimizing the distance vs. load and hop count, etc. The computational complexity of QGE-K is $O(K \times N^2)$. The simulations show improved lifetime and energy performance in comparison with CS-K, GA-UCR and QGA protocols [55]. For environmental monitoring applications where long-term energy conservation is prioritized over strict latency requirements, QGE-K can employ lower cluster-head rotation frequency and stronger energy-weight coefficients to maximize network stability and lifetime.

The second protocol, FEQA, uses fuzzy inference and quantum annealing to facilitate the efficient selection of CHs and the routing of data in extensive networks. The candidate CHs of the nodes are computed as fuzzy variables, which consist of residual energy, degree of nodes, and distance of the nodes to the base station. Routing optimization is performed through an efficient Hamiltonian-based quantum annealing. The overall time complexity is $O(K \times N^2)$. Simulation results show that FEQA outperforms OAFS-IMFO, FC-RBAT, FRNSEER and BOA-ACO in terms of length of lifetime and energy consumption. In the Industrial IoT environments where latency and reliability are priorities, FEQA parameters can be adjusted to favor hop-count optimization and link stability instead of purely energy-based routing.

The third protocol, QE-PSCR, optimizes clustering and routing together by mapping both tasks into a single particle representation. Quantum particle swarm dynamics are used, coupled with chaotic initialization and Lévy flight strategies, to improve global search capacity and combat premature convergence. The overall complexity is $O(n^2 + n^2 m)$, and results indicate better performance than LDIWPSO and APSO-NUCR with regard to network lifetime, energy efficiency, and throughput [56]. For military or tactical WSN deployments operating in dynamic or adversarial environments, increasing the Lévy-flight scaling factor and residual-energy weighting can improve robustness, while chaotic initialization supports faster adaptation to topology changes.

Thus, the proposed quantum-inspired protocols improve energy consumption, load balancing, and network lifetime in WSN deployments. Appropriate parameter tuning according to application-specific requirements, such as latency tolerance, duty-cycle policies, interference conditions, and reliability constraints, is essential to achieve optimal performance. These results indicate the potential impact of quantum-inspired optimization techniques in supporting efficient clustering and routing for future large-scale WSN and IoT systems.

6 Conclusion

This study proposed three quantum-inspired clustering and routing WSNs protocols: QGE-K, FEQA, and QE-PSCR. The protocols focus on energy efficiency, load balancing, and network lifetime for any resource-constrained sensor-node. QGE-K adaptively improves clustering using quantum genetic optimization and K-means clustering. Using the current residual energy and the number of one-hop neighbors, the optimum clustering number is determined adaptively, while the cluster head is selected. Simulation results show that QGE-K consumes less network remaining energy and overhead than CS-K, GA-UCR, and QGA. QGE-K protocol increases throughput.

The FEQA applies fuzzy inference and quantum annealing to select cluster-heads and make routing decisions. A fuzzy inference system selects candidate cluster heads based on node energy, node connectivity, distance to base station, and node centrality, while QA is used to select energy-efficient routing paths. Experimental results show that FEQA outperforms OAFS-IMFO, FCERBAT, FRNSEER, BOA-ACO, and QGA-K when it comes to achieving a longer network lifetime and lower energy consumption, especially in larger networks. The QE-PSCR protocol effectively clusters and routes points in the network through quantum particle swarm representation. The protocol tackles the problem of premature convergence using certain chaotic initializations. Lévy flight strategies are then used in the clustering process for a better global

exploration. Simulations show that QE-PSCR outperforms LDIWPSO and APSO-NUCR in terms of lifetime, energy, and throughputs.

Thus, the proposed quantum-inspired techniques not only improve the stability of clustering processes but with the routing of data and energy as well as the consumption of energy tokens, decrease the expense for WSNs. We believe that the classical inspirations taken from quantum physics allow for the conception of stable and clustered routes for future WSNs and subsequently the Internet of Things.

6.1 Future Works

Future work in WSN clustering and routing will also focus on improving the robustness of routing protocols in fast-changing, diverse environments. Our work explicitly addresses a homogeneous-node climate in a static scenario; however, real applications often feature nodes with varied capabilities and a constantly shifting topology. As WSNs integrate ML and intelligent sensing, the demand for adaptive routing protocols is high, as nodes continually change in status, energy, connectivity, etc. Research will push to integrate heterogeneous nodes and mobile stations into the network, and algorithms for clustering and routing, etc., will need to be robust to fast-changing heterogeneous environments and still perform well at scale.

6.2 Limitations

Although this study presents practical techniques for enhancing WSNs using quantum-optimization-based protocols, its research methodology is limited. It uses a simple model with identical sensor nodes in a static environment, which does not capture the complexities of real-world energy routing strategies affected by node heterogeneity, mobility, and dynamic topology. However, these protocols may require modifications and additional testing before they are applicable to WSNs. The study recommends that future work concentrate on heterogeneous node base stations and on more flexible, scalable clustering and routing procedures to ensure that WSNs are reliable in more dynamic environments.

Acknowledgement: The authors want to acknowledge the fund by Princess Nourah bint Abdulrahman University Researchers Supporting Project number (PNURSP2026R346). The authors would also like to acknowledge the support of AIDA Lab CCIS Prince Sultan University, Riyadh, Saudi Arabia, for the APC of this publication.

Funding Statement: This research was funded by Princess Nourah bint Abdulrahman University Researchers Supporting Project number (PNURSP2026R346), Princess Nourah bint Abdulrahman University, Riyadh, Saudi Arabia.

Author Contributions: Conceptualization: Amjad Rehman, Tariq Mahmood; Methodology: Amjad Rehman, Tariq Mahmood, Faten S. Alamri, Muhammad I. Khan; Software: Tariq Mahmood, Muhammad I. Khan; Writing—original draft preparation: Amjad Rehman, Tariq Mahmood, Faten S. Alamri; Writing—review and editing: Faten S. Alamri, Muhammad I. Khan; Visualization & Validation: Tariq Mahmood, Faten S. Alamri, Muhammad I. Khan; Supervision: Amjad Rehman, Faten S. Alamri. All authors reviewed and approved the final version of the manuscript.

Availability of Data and Materials: The data that support the findings of this study are available from the corresponding author upon reasonable request.

Ethics Approval: Not applicable.

Conflicts of Interest: The authors declare no conflicts of interest.

References

1. Lu X, Yang L, Wu Q, Zhu Y, Zou Y, Shi Y. Dynamic layered clustering routing protocol based on hybrid-optimized neural networks for UWSNs. IEEE Internet Things J. 2025;12(11):16155–70. doi:10.1109/jiot.2025.3531980.
2. Ramya R, Brindha DT. A comprehensive review on optimal cluster head selection in WSN-IoT. Adv Eng Softw. 2022;171(2):103170. doi:10.1016/j.advengsoft.2022.103170.
3. Banitalebi Dehkordi A. EDBLSD-IIoT: a comprehensive hybrid architecture for enhanced data security, reduced latency, and optimized energy in industrial IoT networks. J Supercomput. 2025;81(2):359. doi:10.1007/s11227-024-06872-6.
4. Zhou D, Sheng M, Bao C, Wang Y, Li J, Han Z. Mission-driven resource scheduling in satellite-terrestrial networks: from perspective of collaboration and reconfiguration. IEEE Trans Commun. 2025;73(8):6705–19. doi:10.1109/tcomm.2025.3529250.
5. Chaurasia S, Kumar K, Kumar N. MOCRAW: a meta-heuristic optimized cluster head selection based routing algorithm for WSNs. Ad Hoc Netw. 2023;141(4):103079. doi:10.1016/j.adhoc.2022.103079.
6. Arora M, Gupta K. Quantum computational intelligence techniques: a scientometric mapping. Arch Comput Meth Eng. 2025;32(3):1399–425. doi:10.1007/s11831-024-10183-7.
7. Xu L, Wang X, Wang Z, Cao G. Hybrid quantum genetic algorithm for structural damage identification. Comput Meth Appl Mech Eng. 2025;438(9):117866. doi:10.1016/j.cma.2025.117866.
8. Mahmood T, Saba T, Rehman A, Wang Y. Enhancing Industrial Internet of Things performance through deep transfer learning-based neural network digital twin modeling in data-scarce environments. J Ind Inf Integr. 2025;48(1):100956. doi:10.1016/j.jii.2025.100956.
9. Yao Y, Xiao W, Miao P, Chen G, Yang H, Chae CB, et al. UAV-RHS-enabled full-duplex ISAC covert system: robust beamforming and trajectory optimization. IEEE Trans Commun. 2026;74:5637–53.
10. Mahmood T, Li J, Saba T, Rehman A, Ali S. Energy optimized data fusion approach for scalable wireless sensor network using deep learning-based scheme. J Netw Comput Appl. 2024;224:103841. doi:10.1016/j.jnca.2024.103841.
11. Prince B, Kumar P, Singh SK. Multi-level clustering and Prediction based energy efficient routing protocol to eliminate Hotspot problem in Wireless Sensor Networks. Sci Rep. 2025;15(1):1122. doi:10.1038/s41598-024-84596-6.
12. Saranya VG, Karthik S. Bio-inspired intelligent routing in WSN: integrating mayfly optimization and enhanced ant colony optimization for energy-efficient cluster formation and maintenance. Comput Model Eng Sci. 2024;141(1):127–50. doi:10.32604/cmes.2024.053825.
13. Priyadarshi R, Kumar RR. Evolution of swarm intelligence: a systematic review of particle swarm and ant colony optimization approaches in modern research. Arch Comput Meth Eng. 2025;32(6):3609–50. doi:10.1007/s11831-025-10247-2.
14. Jurado-Lasso FF, Jurado JF, Fafoutis X. LEACH-RLC: enhancing IoT data transmission with optimized clustering and reinforcement learning. IEEE Internet Things J. 2025;12(13):23462–78. doi:10.1109/jiot.2025.3552126.
15. Masihi M, Mehranzadeh A, Barati H, Barati A, Chekin M. Proposing a dynamic clustering algorithm to improve routing performance in the Internet of Things. Clust Comput. 2025;28(14):879. doi:10.1007/s10586-025-05616-2.
16. Tan ND, Quy NM, Nguyen VH. EE-AIRP: an AI-enhanced energy-efficient routing protocol for IoT-enabled WSNs. Comput Netw. 2025;273:111770.
17. Hang J, Yang X. Enhancing local attention with global information interaction via progressive cluster propagation. Pattern Recognit. 2026;172(8):112713. doi:10.1016/j.patcog.2025.112713.
18. Yu Y, Jing G, Hong J, Rodríguez-Piñeiro J, Yin X. A novel wireless channel clustering algorithm based on robust mean-shift. IEEE Trans Wirel Commun. 2025;24(6):5213–26. doi:10.1109/twc.2025.3546457.
19. Long X, Cai W, Yang L, Huang H. Improved particle swarm optimization with reverse learning and neighbor adjustment for space surveillance network task scheduling. Swarm Evol Comput. 2024;85(8):101482. doi:10.1016/j.swevo.2024.101482.
20. Alshammri GH. Enhancing wireless sensor network lifespan and efficiency through improved cluster head selection using improved squirrel search algorithm. Artif Intell Rev. 2025;58(3):79. doi:10.1007/s10462-024-11088-4.

21. Li S, Zhou Y, Luo Q. Enhanced multi-object dwarf mongoose algorithm for optimization stochastic data fusion wireless sensor network deployment. Comput Model Eng Sci. 2025;142(2):1955–94. doi:10.32604/cmes.2025.059738.
22. Trigka M, Dritsas E. Wireless sensor networks: from fundamentals and applications to innovations and future trends. IEEE Access. 2025;13:96365–99.
23. Zhang L, Luo C, Ge X, Cao Y, Zhang H, Xin G. Three-dimensional iterative enhancement for coverage hole recovery in underwater wireless sensor networks. J Mar Sci Eng. 2023;11(12):2365. doi:10.3390/jmse11122365.
24. Zhou Z, Abawajy J, Chowdhury M, Hu Z, Li K, Cheng H, et al. Minimizing SLA violation and power consumption in Cloud data centers using adaptive energy-aware algorithms. Future Gener Comput Syst. 2018;86(6):836–50. doi:10.1016/j.future.2017.07.048.
25. Feng S, Li N, Liu K, Li B, Dong C, Wu Q. A cross Q-learning assisted resource allocation for user-centric optical wireless communication networks. IEEE Trans Green Commun Netw. 2025;9(4):2264–78. doi:10.1109/tgcn.2025.3553202.
26. Pandey OJ, Hegde RM. Low-latency and energy-balanced data transmission over cognitive small world WSN. IEEE Trans Veh Technol. 2018;67(8):7719–33. doi:10.1109/tvt.2018.2839562.
27. Witczak D, Szymoniak S. Review of monitoring and control systems based on Internet of Things. Appl Sci. 2024;14(19):8943. doi:10.3390/app14198943.
28. Wang H, Liu K, Wang C, Hu H. Energy-efficient, cluster-based routing protocol for wireless sensor networks using fuzzy logic and quantum annealing algorithm. Sensors. 2024;24(13):4105. doi:10.3390/s24134105.
29. Chauhan SS, Tanwar G, Pinki, Tiwari R, Venkateswaran B, Ahmad W. Data mining-based smart cluster head selection (SCHS) approach for energy efficiency in wireless sensor networks. J Comput Anal Appl. 2024;33(8):2263–72. doi:10.4236/wsn.2012.411039.
30. Saxena P, Singh Bhadauria S. Hardware implementation of fuzzy logic-based energy-efficient routing protocol for environment monitoring application of wireless sensor networks. Int J Commun. 2025;38(8):e70087. doi:10.1002/dac.70087.
31. Tang Q, Nie F. Clustering routing algorithm of wireless sensor network based on swarm intelligence. Wirel Netw. 2024;30(9):7227–38. doi:10.1007/s11276-023-03584-2.
32. Gu X, Wang S, Wei Z, Feng Z. Cluster-based RSU deployment strategy for vehicular ad hoc networks with integration of communication, sensing and computing. J Inf Intell. 2024;2(4):325–38. doi:10.1016/j.jiixd.2024.02.002.
33. Sattibabu G, Ganesan N, Kumaran RS. IoT-enabled wireless sensor networks optimization based on federated reinforcement learning for enhanced performance. Peer Peer Netw Appl. 2025;18(2):75. doi:10.1007/s12083-024-01887-5.
34. Chowdhury A, De D. Energy-efficient coverage optimization in wireless sensor networks based on Voronoi-Glowworm Swarm Optimization-K-means algorithm. Ad Hoc Netw. 2021;122(10):102660. doi:10.1016/j.adhoc.2021.102660.
35. Di Martino F, Sessa S. A novel quantum inspired genetic algorithm to initialize cluster centers in fuzzy C-means. Expert Syst Appl. 2022;191(554):116340. doi:10.1016/j.eswa.2021.116340.
36. Liu Y, Li C, Xiao J, Li Z, Chen W, Qu X, et al. QEGWO: energy-efficient clustering approach for industrial wireless sensor networks using quantum-related bioinspired optimization. IEEE Internet Things J. 2022;9(23):23691–704. doi:10.1109/jiot.2022.3189807.
37. Somula R, Cho Y, Mohanta BK. SWARAM: osprey optimization algorithm-based energy-efficient cluster head selection for wireless sensor network-based internet of things. Sensors. 2024;24(2):521.
38. Poggiali A, Berti A, Bernasconi A, Del Corso GM, Guidotti R. Quantum clustering with k-Means: a hybrid approach. Theor Comput Sci. 2024;992(7671):114466. doi:10.1016/j.tcs.2024.114466.
39. Hu H, Guo Y, Wang C, Gao D, Liu Q. Optimal relay angle-based clustering routing protocol for wireless sensor networks. J Sens. 2022;2022:5751155. doi:10.1155/2022/5751155.

40. Wang C, Hu Q, Yao H, Wang S, Pei Z. Deciphering a million-plus RSA integer with ultralow local field coefficient h and coupling coefficient J of the Ising model by D-wave 2000Q. Tsinghua Sci Technol. 2024;29(3):874–82. doi:10.26599/tst.2023.9010059.
41. Choudhary S, Sugumaran S, Belazi A, El-Latif AAA. Linearly decreasing inertia weight PSO and improved weight factor-based clustering algorithm for wireless sensor networks. J Ambient Intell Humaniz Comput. 2023;14(6):6661–79. doi:10.1007/s12652-021-03534-w.
42. Guo X, Ye Y, Li L, Wu R, Sun X. WSN clustering routing algorithm combining sine cosine algorithm and lévy mutation. IEEE Access. 2023;11(8):22654–63. doi:10.1109/access.2023.3252027.
43. Mishra SD, Verma D. Energy-efficient and reliable clustering with optimized scheduling and routing for wireless sensor networks. Multimed Tools Appl. 2024;83(26):68107–33. doi:10.1007/s11042-024-18623-z.
44. Karpurasundharapondian P, Selvi M. A comprehensive survey on optimization techniques for efficient cluster based routing in WSN. Peer Peer Netw Appl. 2024;17(5):3080–93. doi:10.1007/s12083-024-01678-y.
45. Gunjan, Sharma AK, Verma K. GA-UCR: genetic algorithm based unequal clustering and routing protocol for wireless sensor networks. Wirel Pers Commun. 2023;128(1):537–58. doi:10.1007/s11277-022-09966-7.
46. Hu B, Tong Y. Cluster routing protocol of wireless sensor network based on virtual cluster heads and improved differential evolution algorithm. In: Proceedings of the 2024 9th International Conference on Cyber Security and Information Engineering; 2024 Sep 15–17; Kuala Lumpur, Malaysia. p. 41–50. doi:10.1145/3689236.3689263.
47. Zhou Z, Shojafar M, Alazab M, Abawajy J, Li F. AFED-EF: an energy-efficient VM allocation algorithm for IoT applications in a cloud data center. IEEE Trans Green Commun Netw. 2021;5(2):658–69. doi:10.1109/tgcn.2021.3067309.
48. Zhao X, Ren S, Quan H, Gao Q. Routing protocol for heterogeneous wireless sensor networks based on a modified grey wolf optimizer. Sensors. 2020;20(3):820. doi:10.3390/s20030820.
49. Shahzad MK, Riazul Islam SM, Hossain M, Abdullah-Al-Wadud M, Alamri A, Hussain M. GAFOR: genetic algorithm based fuzzy optimized re-clustering in wireless sensor networks. Mathematics. 2021;9(1):43. doi:10.3390/math9010043.
50. Maheshwari P, Sharma AK, Verma K. Energy efficient cluster based routing protocol for WSN using butterfly optimization algorithm and ant colony optimization. Ad Hoc Netw. 2021;110(20):102317. doi:10.1016/j.adhoc.2020.102317.
51. Jagadeesh S, Muthulakshmi I. A novel oppositional artificial fish swarm based clustering with improved moth flame optimization based routing protocol for wireless sensor networks. Energy Syst. 2022. doi:10.1007/s12667-022-00534-3.
52. Lipare A, Edla DR, Dharavath R. Energy efficient fuzzy clustering and routing using BAT algorithm. Wirel Netw. 2021;27(4):2813–28. doi:10.1007/s11276-021-02615-0.
53. Tian Z, Huang X, Chen J. Analysis of routing algorithm for smart grid optical communication network based on cloud computing. In: Proceedings of the Third International Conference on Algorithms, Microchips, and Network Applications (AMNA 2024); 2024 Mar 8–10; Jinan, China. p. 295–301. doi:10.1117/12.3032064.
54. Chandrasekaran SK, Rajasekaran VA. Energy-efficient cluster head using modified fuzzy logic with WOA and path selection using enhanced CSO in IoT-enabled smart agriculture systems. J Supercomput. 2024;80(8):11149–90. doi:10.1007/s11227-023-05780-5.
55. Lasser C, Lubich C. Computing quantum dynamics in the semiclassical regime. Acta Numer. 2020;29:229–401. doi:10.1017/s0962492920000033.
56. Martoňák R, Santoro GE, Tosatti E. Quantum annealing by the path-integral Monte Carlo method: the two-dimensional random Ising model. Phys Rev B. 2002;66(9):094203. doi:10.1103/physrevb.66.094203.